The Relative Importance of Solar and Anthropogenic Forcing of Climate Change between the Maunder Minimum and the Present

DAVID RIND, DREW SHINDELL, JUDITH PERLWITZ, AND JEAN LERNER

Goddard Institute for Space Studies, Columbia University, New York, New York

PATRICK LONERGAN

SGT Corporation, New York, New York

JUDITH LEAN

Naval Research Laboratories, Washington, D.C.

CHRIS MCLINDEN

Meteorological Service of Canada, Downsview, Ontario, Canada

(Manuscript received 7 April 2003, in final form 12 September 2003)

ABSTRACT

The climate during the Maunder Minimum is compared with current conditions in GCM simulations that include a full stratosphere and parameterized ozone response to solar spectral irradiance variability and trace gas changes. The Goddard Institute for Space Studies (GISS) Global Climate/Middle Atmosphere Model (GCMAM) coupled to a *q*-flux/mixed-layer model is used for the simulations, which begin in 1500 and extend to the present. Experiments were made to investigate the effect of total versus spectrally varying solar irradiance changes; spectrally varying solar irradiance changes on the stratospheric ozone/climate response with both preindustrial and present trace gases; and the impact on climate and stratospheric ozone of the preindustrial trace gases and aerosols by themselves. The results showed that 1) the Maunder Minimum cooling relative to today was primarily associated with reduced anthropogenic radiative forcing, although the solar reduction added 40% to the overall cooling. There is no obvious distinguishing surface climate pattern between the two forcings. 2) The global and tropical response was greater than 1°C, in a model with a sensitivity of 1.2°C $(W\ m^{-2})^{-1}$. To reproduce recent low-end estimates would require a sensitivity one-fourth as large. 3) The global surface temperature change was similar when using the total and spectral irradiance prescriptions, although the tropical response was somewhat greater with the former, and the stratospheric response greater with the latter. 4) Most experiments produce a relative negative phase of the North Atlantic Oscillation/Arctic Oscillation (NAO/AO) during the Maunder Minimum, with both solar and anthropogenic forcing equally capable, associated with the tropical cooling and relative poleward Eliassen–Palm (EP) flux refraction. 5) A full stratosphere appeared to be necessary for the negative AO/NAO phase, as was the case with this model for global warming experiments, unless the cooling was very large, while the ozone response played a minor role and did not influence surface temperature significantly. 6) Stratospheric ozone was most affected by the difference between present-day and preindustrial atmospheric composition and chemistry, with increases in the upper and lower stratosphere during the Maunder Minimum. While the estimated UV reduction led to ozone decreases, this was generally less important than the anthropogenic effect except in the upper midstratosphere, as judged by two different ozone photochemistry schemes. 7) The effect of the reduced solar irradiance on stratospheric ozone and on climate was similar in Maunder Minimum and current atmospheric conditions.

1. Introduction

The Maunder Minimum time period (approximately 1645–1715) has long been viewed as the most likely recent instance of reduced solar activity producing a noticeable effect on the climate system. The general coldness of the Little Ice Age is reflected in some paleoclimate records for this time period. For example, tree-ring data from northern North America (Jacoby and D'Arrigo 1989) is but one example of a myriad of records indicating the relative coldness of the temperatures during the seventeenth century. Recently, several reconstructions using principal component analysis have

Corresponding author address: Dr. David Rind, Goddard Institute for Space Studies, Columbia University, 2880 Broadway, New York, NY 10025.
E-mail: drind@giss.nasa.gov

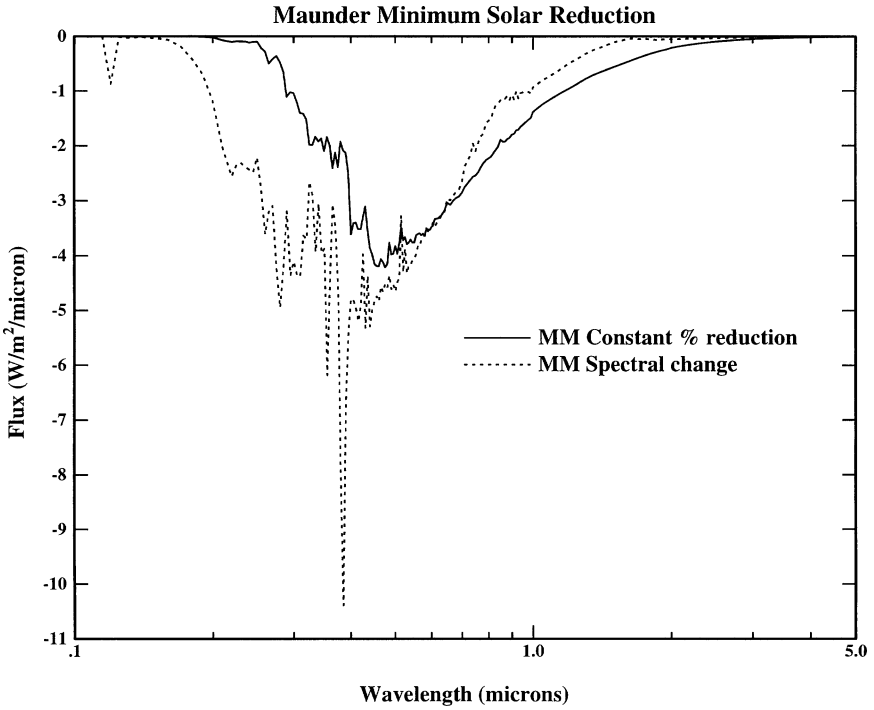

FIG. 1. Input solar irradiance change as a function of wavelength for a 0.2% total energy reduction. Values are shown for both a flat percentage reduction, and with the spectral change from Lean (2000).

questioned whether this time period was really much colder than surrounding periods (D'Arrigo et al. 1999; Mann et al. 1998, 1999); in these reconstructions the hemispheric average response during the Maunder Minimum is only a few tenths of a degree colder than the warmest preindustrial time for the last 300 years, and no different from the temperatures during the late 1880s. Overall, the estimate from these reconstructions is that the global or Northern Hemisphere (NH) temperature was some 0.5°C colder than today, close to 1°C in the extratropics, and just a few tenths of a degree Celsius in the Tropics. Other estimates give values close to twice as large [see the range of estimates from different researchers shown by Briffa and Osborn (2002) and Mann et al. (2003)].

The late seventeenth century was also characterized by a lack of visible sunspots (Eddy 1976). Interpretation of this lack as indicative of reduced solar activity has been suggested by the increased concentration of ^{14}C and ^{10}Be at this time (McHargue and Damon 1991; Stuiver and Braziunas 1993; Beer et al. 1994; Lean and Rind 1998); with reduced solar activity, there is a more quiescent heliospheric magnetic field, with less shielding of the galactic cosmic rays

TABLE 1. List of experiments.

Run	Description
1) CONT	Control with current solar irradiance and atmospheric composition, ozone specified at current day values. Two 500-yr simulations.
2) OCONT	As in 1 except ozone is calculated. Two 500-yr simulations.
3) TOT	Varying total solar irradiance, current-day trace gases and ozone. Two 500-yr experiments (1500–1998), and five 50-yr experiments (1651–1700).
4) SPEC	Varying spectral irradiance, current-day trace gases, and ozone. Two 500-yr experiments (1500–1998), and five 50-yr experiments (1651–1700).
5) SPDO	As in 4 except ozone is calculated. Two 500-yr experiments (1500–1998), and five 50-yr experiments (1651–1700).
6) SPIO	As in 5 except ozone is calculated with preindustrial trace gases. Two 500-yr experiments (1500–1998), and five 50-yr experiments (1651–1700).
7) SPIOC	As in 6 except the preindustrial trace gases and aerosols also affect climate. Two 500-yr experiments (1500–1998).
8) PIOC	As in 7 except the solar irradiance is returned to present-day values. Two 500-yr experiments (1500–1998).

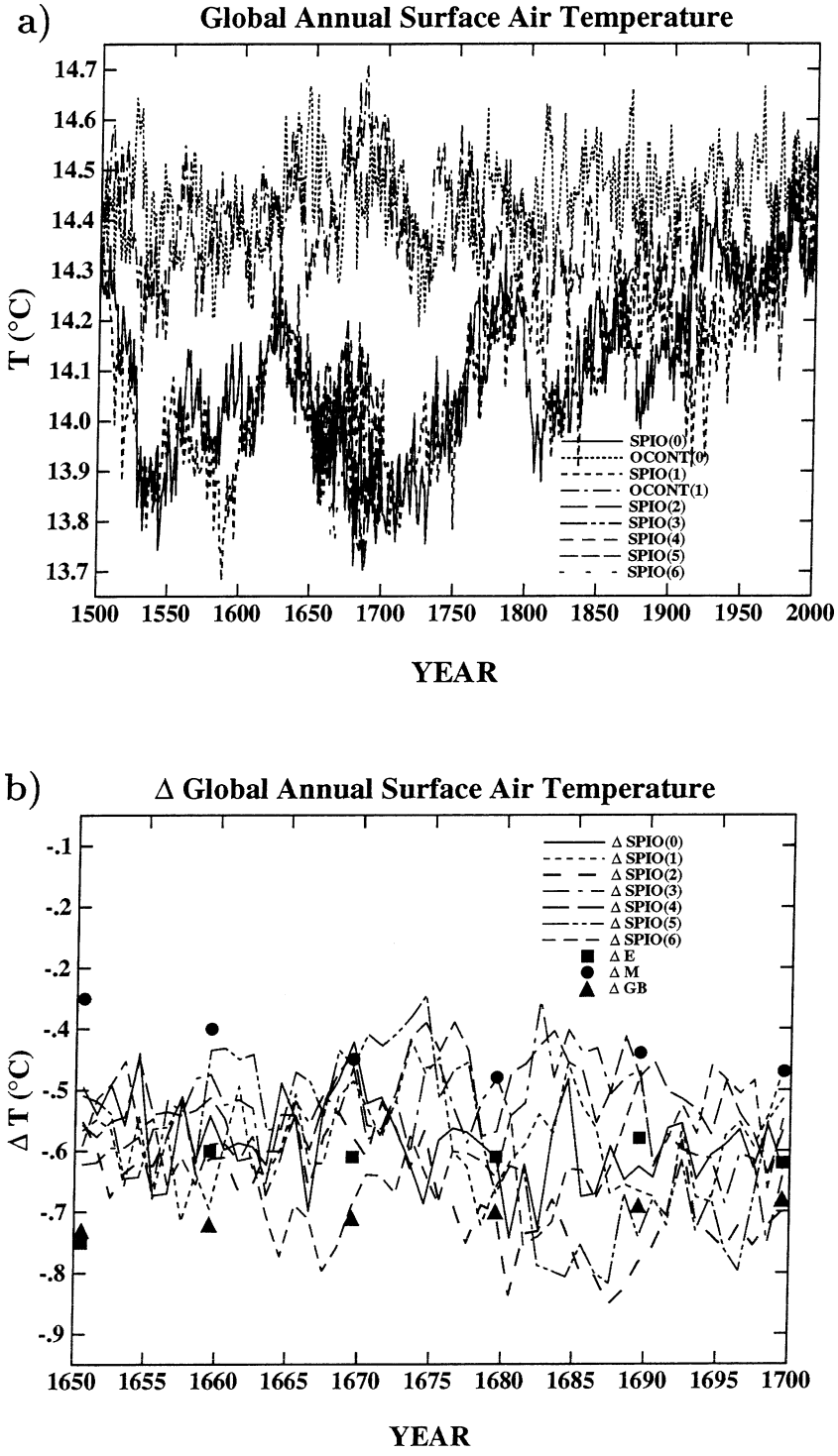

FIG. 2. (a) Global, annual average surface air temperature change for the two control simulations with 1998 solar irradiance and current-day atmospheric composition, and for experiment SPIO (spectral irradiance change plus preindustrial ozone), including the two 500-yr simulations and the five simulations starting from 1651. (b) Differences between the various SPIO experiments and the control run for the 1651–1700 year time period. Shown for comparison are three estimates of the observed temperature change for six times during this period, using a 50-yr smoothing (adopted from Briffa and Osborn 2002). Here E are the results from Esper et al. (2002; for 20°–90°N during the growing season), M are from Mann et al. (1999; annual values for the Northern Hemisphere), and GB are the gridded borehole temperature changes, as shown in Briffa and Osborn (2002). In the GCM, the SH cooling is about 8% larger than in the NH.

generating these isotopes. Estimates of the effect of this reduced activity on total solar irradiance variations ranges from 0.2% (Lean 2000) to as high as 0.4% (Hoyt and Schatten 1993). The Lean reconstruction includes hypothesized changes in the active network radiation, while that of Hoyt and Schatten includes additional changes in temperature and solar luminosity reflected in, for example, changes in solar cycle length. However, Foukal and Milano (2001) argue that not even the network radiation change is valid, and so only the sunspot blocking and faculae emissions effects observed over the last few decades are proven; hence, the irradiance reduction during the Maunder Minimum may only be equivalent to contemporary solar minima, about 0.05%. Lean et al. (2002) also found that solar activity variations can affect the heliospheric magnetic field and hence alter galactic cosmic ray fluxes without necessarily altering total solar irradiance. This raises questions about the relationship between solar irradiance and cosmogenic proxies.

Most previous climate model experiments investigating the potential climatic effect of such irradiance reductions have altered the incoming radiation by a fixed percentage in the 0.2%–0.4% range, and have used models capped at 10 mb (e.g., Rind and Overpeck 1994; Rind et al. 1999; Cubasch et al. 1997). The resultant cooling was on the order of 0.4°–0.5°C relative to today. The time period also contained preindustrial trace gases and aerosols, which, using current estimates, imply a forcing of between 1 and 2 W m^{-2} from the preindustrial to the present, depending on the magnitude of the indirect effect of aerosols on cloud cover. This can be compared with the estimated solar forcing contribution discussed above of 0.18–1.4 W m^{-2} (0.05%–0.4%). Based on the relative forcings, the solar contribution to the difference between the Maunder Minimum time period and today (i.e., 1998 solar irradiance) may, at one extreme, be due equally to solar and anthropogenic forcing, or, at the other extreme due primarily to anthropogenic effects, 10 times larger than the solar effect. [Note that this is in contrast to the cooling of the Maunder Minimum time period relative to the contiguous preceding and following preindustrial times, when solar irradiance may have changed but atmospheric composition had not, e.g., Houghton et al. (2001), their Fig. 3.2]. The possibility that volcanic aerosols were also different in this time period is another complication, which will be discussed more fully below.

If the spectral irradiance change between solar maximum and solar minimum conditions is any guide to what would have happened with a complete lack of sunspot activity for an extended time period, then it is likely that the greatest irradiance changes occurred in the ultraviolet radiation or shorter wavelengths (Lean 2000) that are absorbed in the stratosphere. With the same total irradiance reduction, this would imply less change in the visible and near-infrared radiation that are absorbed in the troposphere or at the surface. As one focus, we test the effect of proposed alterations in the solar spectrum in comparison with fixed percentage total solar irradiance changes for the Maunder Minimum time period.

Stratospheric ozone appears to vary with the solar cycle (McCormack and Hood 1996), with greater ozone, especially in the upper stratosphere, during solar maximum conditions. To the extent that spectral irradiance changes accompanied the Maunder Minimum, they likely affected stratospheric ozone. How this may have altered the climate system is the second focus of this paper.

Both of these simulations are compared with experiments in which preindustrial anthropogenic trace gas and aerosols changes are included. This allows for a direct comparison of anthropogenic versus solar forcing, and represents a third focus.

In order for the effect of ozone to be simulated in the model, a full stratosphere is required. The simulations described in this paper utilize the Goddard Institute for Space Studies Global Climate/Middle Atmosphere Model (GCMAM; Rind et al. 1988) which extends to an altitude of 85 km. In addition to allowing for an ozone response, Shindell et al. (1999a) showed that lifting the upper boundary of the model above the stratosphere in the GISS GCM was necessary to better simulate the effect of climate change on the first EOF of the sea level pressure field, the so-called Arctic Oscillation. Therefore an additional advantage to using this version of the GISS model is the capability of assessing how the normal modes may have varied in the Maunder Minimum relative to today. As an additional focus, we compare the results of this model to our studies, which used the model having a top at 10 mb (Rind and Overpeck 1994; Rind et al. 1999).

2. Model and experiments

The GISS GCMAM has 23 vertical layers between the surface and the mesopause, with $8° \times 10°$ (latitude $\times$ longitude) resolution. It is connected to a *q*-flux mixed-layer ocean, in which heat transport is prescribed and unchanged through the course of the experiment, and vertical heat diffusion occurs through the bottom of the mixed layer (Hansen et al. 1984). This configuration allows the numerous multicentury runs needed for this paper to be conducted using available resources. In the transient climate-change mode the model has been previously run for climate simulations of the twenty-first century (e.g., Shindell et al. 1999a). It has a relatively high climate sensitivity, on the order of 1.2°C $(W\ m^{-2})^{-1}$ (Rind et al. 1998). The model appears capable of simulating some components of the dynamic response to solar cycle variations (Shindell et al. 1999b, 2001b).

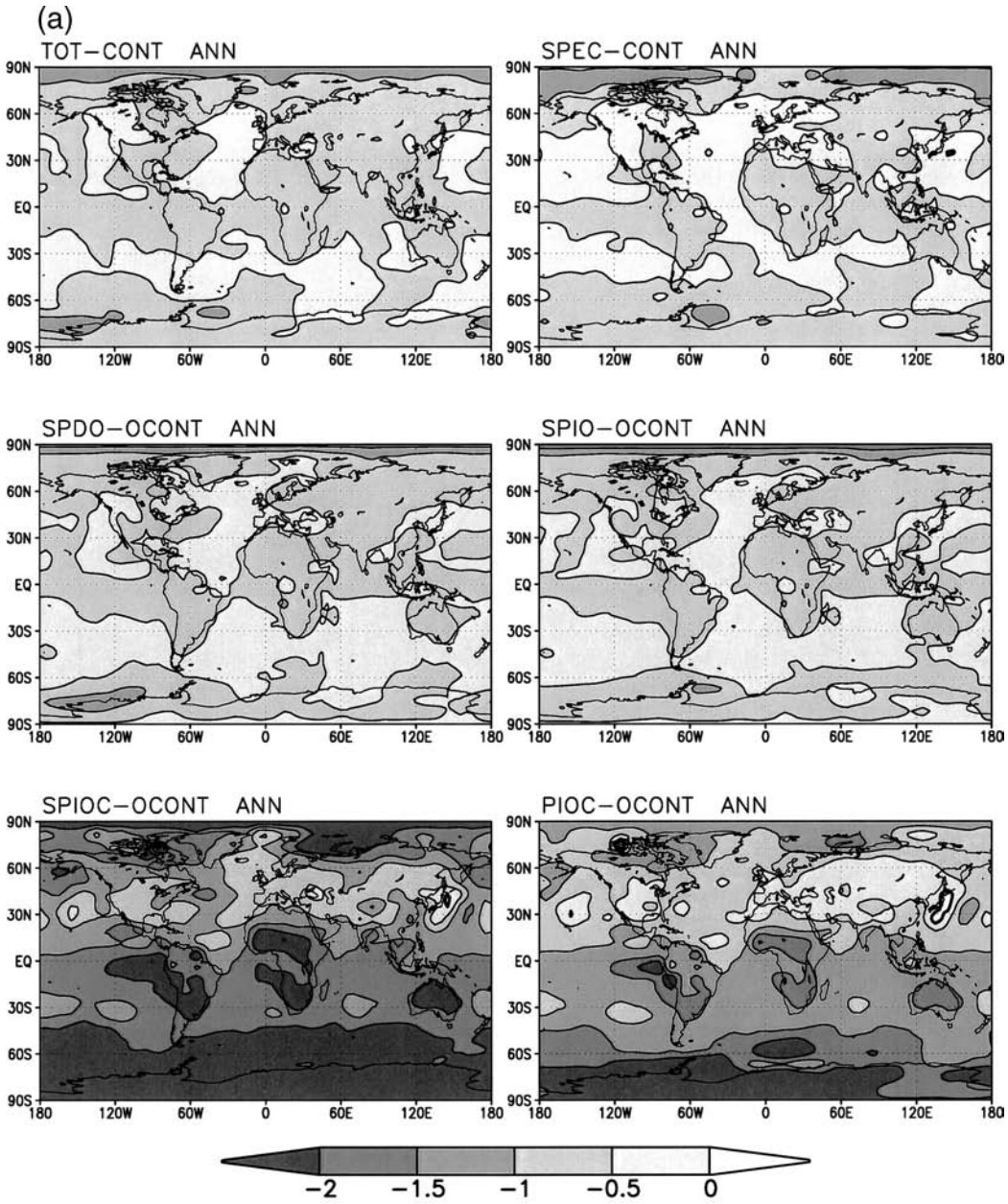

FIG. 3. Surface air temperature change for the (a) annual average and (b), (c) solstice seasons in the different experiments. For this and the other figures, results are given for the period 1651–1700 of the ensemble of simulations for each experiment compared to the mean of their respective control runs. All the changes are significant at the 95% level, except for the occasional small warming regions at high latitudes.

The simulations includes parameterizations that calculate the response of stratospheric ozone to variations in solar irradiance (particularly UV), overhead ozone column, temperature, water vapor, chlorine, and N_2O (HO_x, NO_x, and ClO_x). This work, based on an offline 2D photochemical model is discussed in more detail in Shindell et al. (1999b, 2001a). It does not allow for advection of the ozone changes, or for advection changes to alter ozone (except through their effect on temperature). Its economy is again important for the long simulations discussed here.

In addition, as a check on the ozone change results, we repeated several of the experiments with a $4° \times 5°$ (latitude $\times$ longitude), 53-layer version of the model incorporating online ozone advection with the linearized photochemistry scheme (Linoz) of McLinden et al. (2000).

The solar irradiance variations employed in these

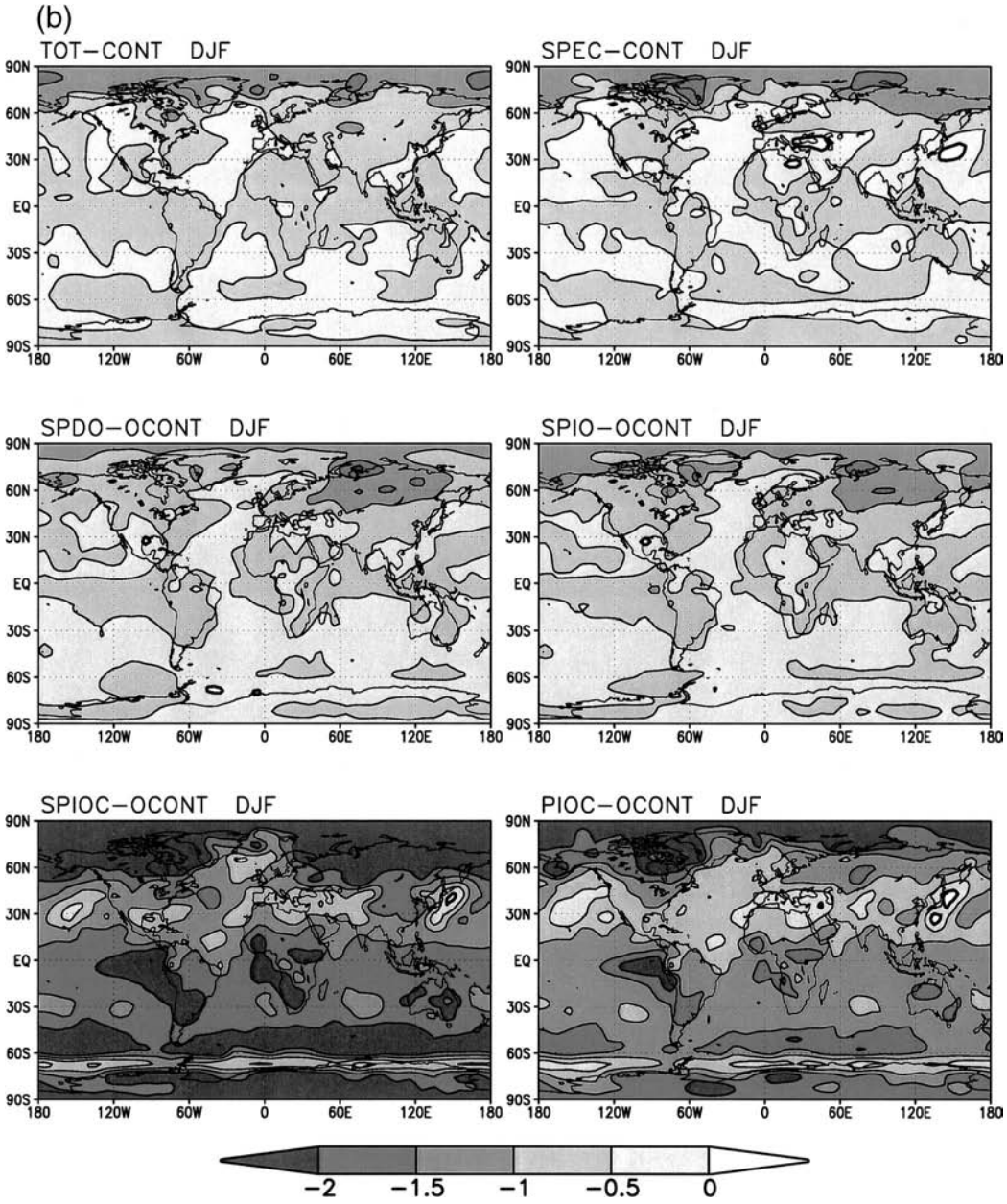

FIG. 3. (*Continued*)

experiments, both total and spectral, were developed by Lean (2000). They are based on a comparison of solar cycle variations to observed differences using broadly defined sunlike stars. During the Maunder Minimum the total irradiance change is estimated in this reconstruction to be 0.2%. It is applied in two ways: as a constant percentage reduction, and in a spectrally varying form. The differences are shown in Fig. 1. Clearly the spectrally varying change has greater reduction in UV radiation, while less in the near-IR portion of the spectrum.

The following runs are discussed in this paper. 1) A control run (CONT) which uses current solar irradiance (for 1998, hence representing conditions in between solar maximum and solar minimum) and current trace gases. 2) A control run with the same solar and atmospheric configuration but in addition the ozone is calculated (OCONT). This is for comparison with the climate change runs in which ozone is calculated. 3) A simulation using total solar irradiance variations (TOT), with a fixed percentage change at all wavelengths. It uses current trace gas composition. 4) A simulation allowing the solar spectrum to vary as well (SPEC), with the integrated solar irradiance

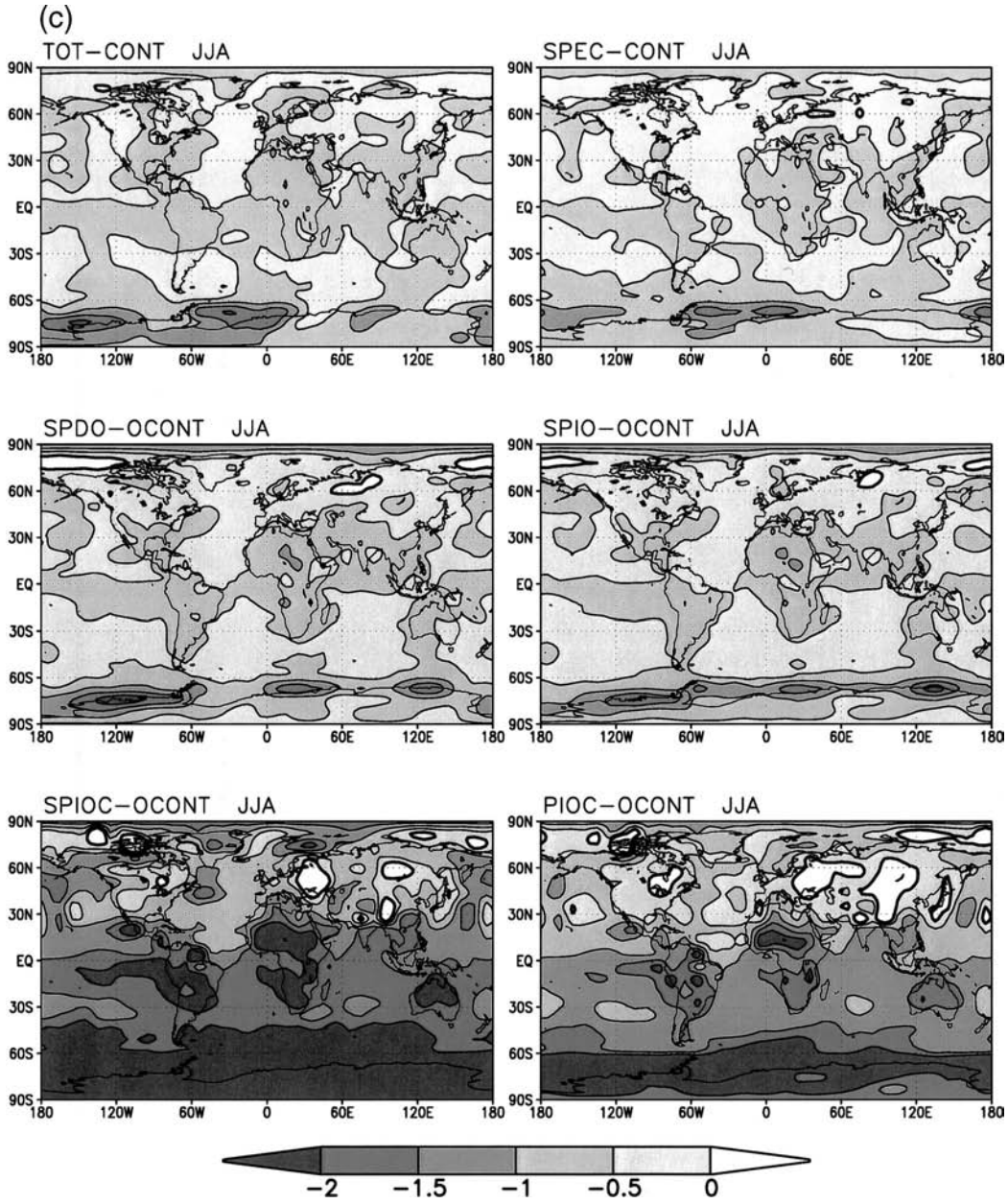

FIG. 3. (*Continued*)

change the same as in run 3. It also uses current atmospheric composition. 5) As in experiment 4 except that ozone is allowed to respond, using current atmospheric composition [solar plus present-day ozone (SPDO)]. (6) As in experiment 5 except that for the ozone calculation, preindustrial trace gas composition is assumed [hence solar plus preindustrial ozone (SPIO)]. This includes methane reduced to 37% of its current value, N_2O reduced by 18%, water vapor reduced by 27% (from the reduced methane values), and no chlorofluorocarbons (CFCs). 7) As in experiment 6, except that the preindustrial trace gases (including CO_2 reduced to 280 ppm) and tropospheric aerosols also affect the radiation and hence the *climate* directly (SPIOC). Finally, 8) the same configuration as in 7) except solar irradiance is returned to current values (PIOC). Table 1 provides a complete list of these experiments and the simulation periods.

The difference between TOT and CONT and SPEC and CONT indicates the effect of total or spectrally varying irradiance on the Maunder Minimum climate relative to today. The difference between runs SPDO and OCONT, or SPIO and OCONT, shows the effect of allowing ozone to respond, in addition to solar

TABLE 2. Change in various globally, annual averaged parameters affecting the radiation balance in the different experiments. Results from the ensemble of simulations for each experiment for the years 1651–1700 are compared to their respective control runs for the same 50-yr period. Std devs from the ensemble runs from the different experiments are given in parentheses for selected quantities, and SW and LW stand for shortwave and longwave, respectively.

Parameter/run	TOT	SPEC	SPDO	SPIO	SPIOC	PIOC
ΔSW incident at TOA (W m^{-2})	−0.7	−0.7	−0.7	−0.7	−0.7	0
ΔLW initially (W m^{-2})	0	0	0	0	−1.9	−1.9
ΔSW absorbed in stratosphere (W m^{-2})	−0.02	−0.11	−0.14	0.07	−0.03	0.12
ΔOzone at 0.68 mb (%)	0	0	−1.90 (.04)	11.9 (.05)	7.56 (.5)	10.23 (0.1)
ΔTotal ozone (%)	0	0	−1.4 (.01)	2.7 (.02)	2.0 (.01)	3.4 (0.32)
ΔSW incident at tropopause (W m^{-2})	−0.68	−0.59	−0.56	−0.77	−0.67	−0.14
ΔSW reflected in troposphere (W m^{-2})	0.17	0.17	0.34	0.20	−0.07	−0.02
ΔSW absorbed in troposphere (W m^{-2})	−0.38	−0.39	−0.46	−0.37	−0.87	−0.47
ΔSW incident at surface (W m^{-2})	−0.50 (.09)	−0.45 (.11)	−0.50 (.09)	−0.60 (.05)	0.05 (.07)	0.35 (0.07)
ΔSW absorbed at surface (W m^{-2})	−0.70 (.14)	−0.70 (.13)	−0.60 (.11)	−0.70 (.07)	−0.90 (.14)	−0.30 (0.01)
ΔGlobal surface air temperature (°C)	−0.56 (.07)	−0.55 (0.1)	−0.53 (.06)	−0.55 (.05)	−1.65 (.06)	−1.11 (0.06)
Ratio Δ surface air temperature Tropics (30°N–30°S)/extratropics	1.14 (.12)	0.90 (.1)	0.96 (.05)	0.93 (.07)	0.95 (.04)	1.01 (.09)
ΔGlobal air temperature (°C)	−0.71 (.08)	−0.67 (.13)	−0.69 (.08)	−0.61 (.07)	−1.74 (.06)	−1.12 (.02)
ΔGlobal air temperature @ 272 mb	−0.85 (.08)	−0.75 (.13)	−0.80 (.11)	−0.80 (.07)	−2.15 (.07)	−1.5 (.01)
ΔGlobal air temperature @ 0.68 mb	−0.15 (0)	−1.0 (.07)	−1.6 (.04)	0.70 (.06)	3.25 (.07)	4.75 (.07)
ΔWater vapor (%)	−4.4 (.44)	−3.8 (.74)	−4.1 (.57)	−4.1 (.44)	−11.6 (1.6)	−8.0 (1.3)
ΔSea ice cover (% absolute)	0.10 (0)	0.15 (.05)	0.10 (.05)	0.10 (.05)	0.75 (.07)	0.55 (.07)
ΔGround albedo (% absolute)	0.11 (.02)	0.13 (.03)	0.10 (.01)	0.10 (.01)	0.47 (.05)	0.31 (.06)
ΔHigh cloud cover (% absolute)	−0.15 (0)	−0.10 (0)	−0.10 (0)	−0.2 (0)	0.3 (0.3)	0 (.14)
ΔLow cloud cover (% absolute)	0.22 (.05)	0.20 (.08)	0.25 (.08)	0.3 (.07)	0.95 (.07)	0.70 (.01)
ΔPlanetary albedo (% absolute)	0.14 (.04)	0.17 (.06)	0.19 (.04)	0.15 (.03)	0.37 (.03)	0.18 (.01)
ΔGreenhouse effect (W m^{-2})	−1.95 (.27)	−1.85 (.25)	−1.65 (.20)	−1.75 (.20)	−5.9 (1.4)	−4.3 (1.7)
ΔGreenhouse efficiency (×10^{-4})	−19 (3)	−15 (3)	−14 (2)	−17 (2)	−63 (10)	−48 (5)
ΔNet radiation at TOA (W m^{-2})	−0.09 (.04)	−0.08 (.05)	−0.14 (.04)	−0.15 (0)	−0.25 (.07)	−0.2 (0)

irradiance changes, while the difference between SPDO and SPIO indicates the effect of changing atmospheric composition between preindustrial times and today on the ozone response. Run SPIOC minus run OCONT represents the climate change between the Maunder Minimum and today when both solar and trace gas/aerosol changes are included. Finally, PIOC minus OCONT indicates how much the trace gas and tropospheric aerosol changes have affected climate by themselves.

Each experiment and control run was run for 500 years starting from 1500 A.D. The initial atmospheric conditions at 1500 were then altered and each experiment/control was repeated. Since the emphasis here is on the 50-yr averages, 1651–1700, we then ran most of the experiments 5 more times for that interval, varying the initial atmospheric conditions but starting with the sea surface temperatures generated from one of the 500-yr runs. An example is given in Fig. 2a, which shows the change of global, annual surface air temperature as a function of time in the experiment with the spectral irradiance change and preindustrial ozone (SPIO). Given are the two control run values, the two 500-yr simulations of SPIO, and the five ensemble runs for the 1650–1700 time period. Shown in Fig. 2b are the differences of each of these runs from the control run for the time period of interest here. Unless otherwise stated, results shown in the following figures and tables use the full ensemble of simulations for each experiment (i.e., generally seven runs) minus the average of the two control runs for the same time period. Significance is determined by comparison with the interannual standard deviations from the respective control runs.

To validate the approach of starting some of the runs in 1651, we need to determine if the potential cooling during the Maunder Minimum time period is driven primarily by prospective solar irradiance changes during 1651–1700, or by changes originating in the climate system prior to this time (i.e., the ''committed cooling'' resulting from the forcing imposed before 1650). As shown in Rind et al. (1999), the solar irradiance reconstruction has reduced values (relative to today) continually from 1500 to 1700. If most of the cooling during the Maunder Minimum is generated from the reduced irradiance prior to 1650, due to the slow response time of the system, then the additional runs made starting in 1650 will only contain a small portion of the variability.

We test how much of the cooling is due to the actual solar reduction within the 50-yr time frame in the following way. For the two experiments starting in 1500, the global surface air temperature cooling averaged for the period 1651–1700 relative to the present was 0.53°C, the same value actually occurring in each experiment. We ran another experiment starting from 1651 with the initial sea surface temperatures set at the 1651 values

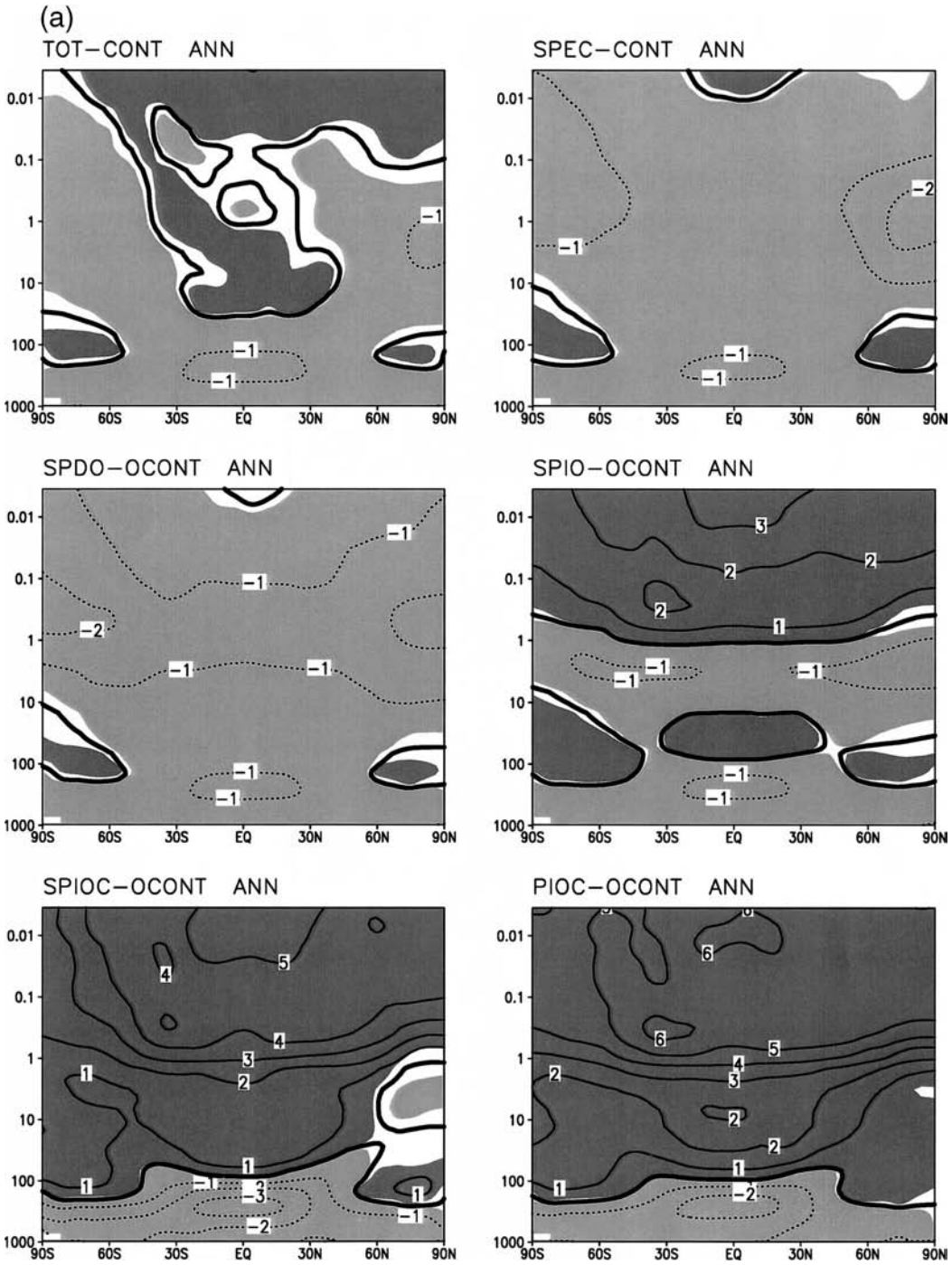

FIG. 4. Zonal average temperature changes for (a) annual average and (b) Dec–Feb (DJF) in the different experiments. Significant changes (at the 95% level) are shown by the dark shading for temperature increases, and lighter shading for temperature decreases.

generated by one of these runs; however, now we returned the solar irradiance to current day values. If the cooling was mostly from the prior irradiance change, an effect already encompassed in the 1651 SSTs, using the current solar irradiance should not have diminished the cooling response. However, with the current irradiance the average cooling for the 50 yr from 1651 to 1700 was just 0.08°C compared to the control run for this time period (and thus not significant). We conclude that the model cooling during the Maunder Minimum arose primarily from the solar changes within that 50-yr time period.

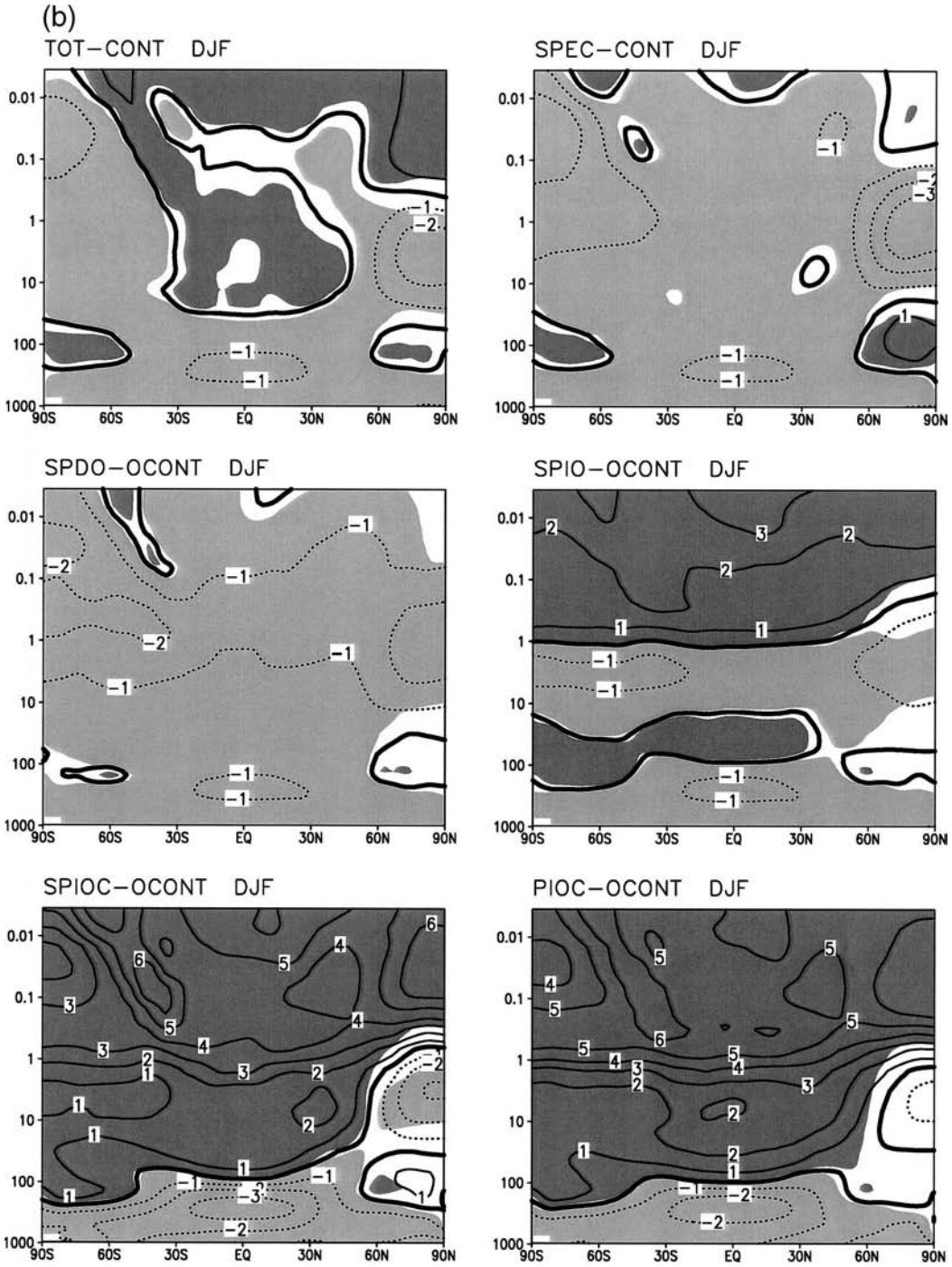

FIG. 4. (*Continued*)

3. Results

For the sake of conciseness with these many experiments, we present the results as answers to the specific questions that motivated our simulations. Additional broader implications are addressed in the discussion section.

a. Question 1: Does using the spectrally differentiated solar irradiance change produce less tropospheric cooling than the total irradiance change (which had the same percentage reduction at each wavelength)?

No.

The control run uses a total solar irradiance of 1367.6 W m^{-2}, and both TOT (total irradiance reduction of 0.2% across the spectrum) and SPEC (spectrally differentiated change) use 1364.8 W m^{-2}. Although both choices lead to the same total energy reduction (0.68 W m^{-2} when spread over the sphere), as shown in Fig. 1 the spectrally varying approach produces more variance (some 25%) in the UV short of 0.4 μm. The UV component of the radiation perturbation primarily affects the stratosphere, and utilizing the spectral variations reduces the total irradiance change entering into the troposphere.

The global, annual average changes between experiments TOT and SPEC and CONT are given in Table 2; standard deviations from the seven experiment simulations are given in parentheses. Included in the table are the radiative, climate feedback, and temperature responses. The use of spectral irradiance rather than total irradiance does not result in any difference in global surface temperature cooling; the small difference in radiation change at the tropopause is compensated for by variations in surface albedo, and most of the global climate responses in the two experiments are not significantly different. Several things are significantly different though: the tropical cooling is greater relative to the extratropical (see the ratio in Table 2) with the total solar irradiance reduction; this can also be seen in Fig. 3, which depicts the geographic variation of surface temperature response for the annual average and the two solstice seasons. The greater extratropical cooling with the spectral discrimination is responsible for the slightly larger sea ice change, and the slightly greater surface albedo increase. Also, temperature reduction at 0.68 mb (~50 km; Table 2) is much larger when the spectral irradiance change was used due to its greater UV reduction, and the greater cooling is true for the stratosphere in general, as is shown in Fig. 4. The warming in the tropical stratosphere in TOT is a dynamic feature, discussed next.

b. *Question 2: How does ozone respond to the solar irradiance change?*

Ozone decreases in the midstratosphere, although the effect can be overridden by changes in the background atmospheric composition.

Less UV radiation is expected to produce less ozone, as is observed during contemporary solar minimum conditions and simulated with this model. However, the UV reduction also leads to stratospheric cooling, which increases the ozone photochemical production relative to loss. During the Maunder Minimum time period, with its prescribed greater UV reduction compared to solar minimum conditions currently (a factor of 2 in the Lean estimate), both effects are amplified. Using the current day background atmosphere (SPDO), the solar change reduces ozone in the stratosphere (Table 2; Fig. 5), at all levels extending down to the lower stratosphere. With the preindustrial background atmosphere, (SPIO), ozone increases due to the altered photochemistry except in the midstratosphere, where reduced UV (absorbed at higher levels by the increase ozone) and the solar variability-induced UV reduction still causes a small decrease.

When the stratosphere is allowed to respond radiatively to the preindustrial atmosphere (SPIOC), the stratosphere warms (due to reduced CO_2), and so the ozone increase is somewhat smaller than in SPIO while the midstratosphere decrease is larger. But without the solar irradiance change (PIOC), the ozone increase is larger, with the small midstratosphere decrease due now entirely to increased UV absorption at higher levels. Hence when the various effects are considered, the UV reduction in the preindustrial atmosphere is causing less ozone compared to today, an effect that is overridden in the upper and lower stratosphere by the effect of the altered atmospheric composition on ozone photochemistry.

c. *Question 3: How does the ozone change affect the climate response?*

It has little effect in the troposphere.

The temperature in the stratosphere clearly responds to the ozone change (e.g., Fig. 4), with greater cooling accompanying the ozone decrease in experiment SPDO, and temperature and ozone increasing in the upper and lower stratosphere in experiment SPIO (both with respect to OCONT). As can be seen in Table 2, the shortwave radiation at the tropopause is somewhat affected. However, the temperatures in the troposphere and at the surface are not significantly different with the ozone change (Table 2 and Figs. 3 and 4; cf. experiments SPEC, SPDO, and SPIO).

The ozone changes will affect longwave radiation as well, theoretically reducing the greenhouse capacity in SPDO, while increasing it in SPIO. Larkin et al. (2000) found that the compensation between shortwave and longwave response limited the solar-induced ozone change radiative effect in the troposphere, at least on the global average. However, as indicated in the table, the greenhouse effect is not significantly different in the two experiments probably due to the tropospheric response. Similarly, the lack of significant ozone impact on tropospheric temperature is likely due to the greater strength of the tropospheric feedbacks to the solar/trace gas forcing compared to the magnitude of the overall ozone radiative perturbation.

d. *Question 4: How does the temperature response to solar forcing compare with that due to the anthropogenic forcing for the Maunder Minimum relative to today?*

With the forcings used here, the anthropogenic effect is 2 times larger.

The relative magnitudes of the forcings are shown in Table 2. The anthropogenic radiative longwave forc-

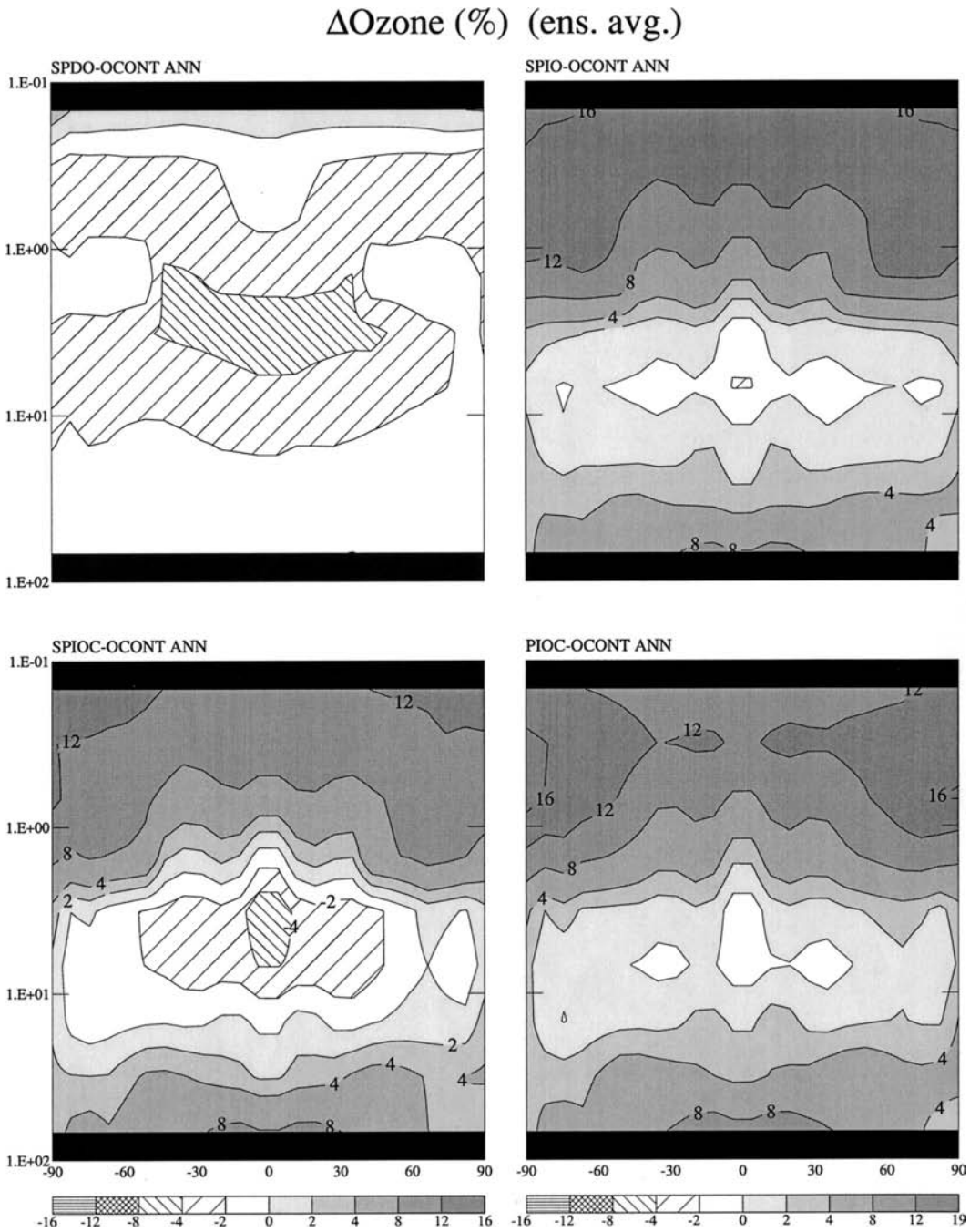

FIG. 5. Percentage change in the annual average stratospheric ozone in the different experiments.

ing in experiments SPIOC and PIOC results from 2.5 W m^{-2} decrease due to preindustrial trace gas decreases (e.g., Houghton et al. 1996) and 0.6 W m^{-2} increase due to reduced aerosols (within the range of the Houghton et al. 1996 estimates). The sum is therefore 2–3 times as large as the assumed solar irradiance reduction. The surface temperature response to the anthropogenic influence is about twice as large as for the solar forcing alone (PIOC versus SPIO), with a more strongly reduced greenhouse effect (longwave energy emitted from the surface minus that leaving the top of the atmosphere) and greenhouse efficiency (greenhouse effect normalized by the surface emissions). When both solar and anthropogenic effects are included, the global surface temperature change is approximately a linear response to each individually (i.e., the change in SPIOC is similar to that of PIOC plus SPIO). This approximate linearity holds for most of the feed-

TABLE 3. Change in high-latitude indices during Northern Hemisphere winter. Values significant at least at the 95% level are shown in boldface.

	TOT	SPEC	SPOD	SPIO	SPIOC	PIOC	−0.25%	−2%
ΔNAO SLP diff (mb)	**−1.09 (−0.28)**	**−0.78 (−0.18)**	**−1.25 (−0.29)**	**−0.79 (−0.18)**	**−2.55 (−0.61)**	**−2.19 (−0.52)**	0.58	**−2.25**
NAO (eof)	**−0.22**	−0.10	**−0.18**	−0.12	**−0.37**	**−0.34**		
ΔSLP (mb) (30°–50°N)–(60°–80°N)	**−0.64 (−0.18)**	−0.10 (−0.08)	**−1.09 (−0.28)**	**−0.73 (−0.19)**	**−2.11 (−0.56)**	**−1.93 (−0.36)**	−0.02	**−2.31**
AO (eof)	**−0.19**	−0.04	**−0.23**	−0.13	**−0.47**	**−0.32**		
Δ500-mb heights (m) (30°–50°N)–(60°–80°N)	−2.3	1.9	**−7.5**	−4.3	−5.5	−6.9	−4	4
Δ100-mb heights (m) (30°–50°N)–(60°–80°N)	**−31**	**−40**	**−33**	**−17**	**−59**	**−36**	−10	**−37**
Δ10-mb heights (m) (30°–50°N)–(60°–80°N)	−20	**−117**	−61	−4	−40	7	NA*	NA*

* NA indicates not applicable.

backs shown in Table 2 as well (water vapor, sea ice, ground albedo, planetary albedo, and low cloud cover), and even for many of the geographic temperature variations (Fig. 3). The linearity implies that the effect of the solar forcing did not depend on the background atmospheric state (i.e., preindustrial versus present day).

e. Question 5: How does the solar forcing and/or ozone response influence the phase of the North Atlantic Oscillation (NAO) or Arctic Oscillation (AO), and does it differ from that due to anthropogenic forcing?

Both the solar and anthropogenic forcings help generate the negative phase of the AO/NAO.

The NAO as well as other high-latitude index changes are indicated in Table 3. The response of the NAO index is calculated in two ways. First, we determined the index based on the sea level pressure difference between the 12 grid points surrounding Portugal and Iceland. Shown are both the pressure difference for the experiment compared to its control run, and the value normalized by the interannual standard deviations of the control run (in parentheses, for comparison with the second approach).

Second, we determined the leading EOF of sea level pressure over the North Atlantic region north of 20°N based on the control runs. The sea level pressure response is projected onto this EOF pattern. The coefficient shown is normalized respective to the interannual standard deviation of the temporal expansion coefficient of the leading EOF.

Similar to the NAO index, the response in the Arctic Oscillation index is determined by using on the one hand the difference between mid- and high-latitude sea level pressures (and its standardized value, in parentheses) and on the other hand the leading EOF of the Northern Hemisphere sea level pressure poleward of 20°N. Values significant at least at the 95% level are shown in boldface type. In order to illustrate the change in the Northern Hemisphere annular mode within the atmosphere, the mid-versus high-latitude height differences are also presented for the 500, 100, and 10-mb levels.

As can be seen in the table, the high-latitude index changes at the surface are negative in the Maunder Minimum relative to today in all of these experiments. The response with the ozone decrease in SPDO is generally significant, while that is not always the case with no ozone response (SPEC) or ozone increases (SPIO). With greater cooling (SPIOC, PIOC), the effect is stronger. The response in the lower stratosphere is also negative, while the changes in the midtroposphere and stratosphere are generally not significant.

The process by which changes in these indices occur is indicated in Figs. 6–8 for December–February (DJF) with the sea level pressure changes themselves given in

Fig. 9. Tropospheric cooling maximizing in the tropical upper troposphere (as shown in Fig. 4b) results in a relative east wind increase (from the thermal wind relationship) in the upper troposphere/lower stratosphere (Fig. 6, shading). The wave energy [Eliassen–Palm (EP)] flux responds with relative poleward refraction circa 100 mb (Fig. 6, arrows), leading to EP flux convergences in the extratropics (Fig. 7). These convergences generate a more direct residual circulation in the troposphere (Fig. 8), which results in rising air at midlatitudes, and sinking air at higher latitudes. The sea level pressure changes (Fig. 9a) reflect this altered vertical circulation pattern, with higher pressure at high latitudes (more so in SPDO), and reductions at midlatitudes. The same effect can be seen in the Southern Hemisphere in both summer and (especially) winter (Fig. 9b). As the upper-tropospheric cooling is stronger with greater cooling, all these effects are stronger in SPIOC and PIOC. The effect is not diminished when only anthropogenic forcing is used (PIOC).

The more direct circulation associated with extratropical EP flux convergences produce subsidence and warming over the poles in the upper troposphere/lower stratosphere (Fig. 4b). This raises the pressure surfaces there and produces the negative high-latitude index effect (Table 3; 100 mb). Relative EP flux divergences occur in most of the experiments in the upper stratosphere (Fig. 7), leading to indirect residual circulation changes (Fig. 8), with relative rising air at high latitudes, and hence cooling in the mid- to upper stratosphere diminishing the high-latitude pattern, at least in significance (Table 3; 10 mb). The tropical residual circulation is reduced as a consequence of the EP flux divergence in the subtropics ~100 mb, and the effect of reduced upwelling in the stratosphere is a relative dynamical warming, see in Fig. 4.

f. Question 6: Does the precipitation pattern show distinct differences between anthropogenic and solar forcing?

No.

The residual circulation change (Fig. 8) also indicates a weakening of the Hadley circulation during DJF, an effect that can also be seen in Fig. 9a with increased sea level pressure in the Tropics, and decreased values in the subtropics. That change does not depend upon the nature of the forcing but is more associated with the overall magnitude of the cooling. A weaker Hadley cell (peaking at about an 8% reduction in SPIOC during DJF) is associated with reduced tropical and greater subtropical precipitation (−16% and +4%, respectively, in SPIOC), which also respond primarily to the magnitude of the Hadley cell change and tropical cooling (and hence is affected by both solar and anthropogenic forcings). Extratropical precipitation changes followed the NAO/AO sea level pressure patterns, thus they also did not discriminate between the forcings outside of their different magnitudes.

In studies with the Universities Global Atmospheric Modelling Programme (UGAMP) GCM (Haigh 1996) and the Met Office's Unified Model (Larkin et al. 2000), the Hadley cell strengthened in solar minimum conditions associated with reduced ozone, although the changes were small (on the order of a few percent). Here the Hadley cell weakening is not noticeably different between SPDO and SPIO despite their different ozone responses, possibly because the effect is driven by the change in tropical sea surface temperatures.

Regional changes in temperature, precipitation, and soil moisture for the annual average are given in Table 4, in which one can compare the solar effect with the anthropogenic effect directly (SPIO and PIOC). In general, the sign of the precipitation and soil moisture changes are similar with the two forcings. The linearity of the response can also be assessed by subtracting the results of PIOC from SPIOC, and comparing them to SPIO. An approximate linear response for temperature appears even at this regional level, and this is true as well for the hydrologic changes when they are significant (which is less often in SPIO with its smaller cooling). Hence, even on the regional level, the solar effect is not dependent on the background state, acting approximately independently from the anthropogenic forcing. Note that Meehl et al. (2003) found that a small amount of anthropogenic forcing (e.g., for the earlier part of the twentieth century) did enable solar forcing to produce some different monsoonal effects than when it acted alone; either this affect is overwhelmed when the stronger greenhouse gas forcing is used, as in these experiments, or it is dependent upon the model's cloud cover scheme.

4. Discussion

In this section we address some broader implications of our results.

a. Causes of the global Maunder Minimum cooling

Our multiple simulations indicate that the adopted solar irradiance reduction produced a 0.5°C global cooling, which was in addition to the approximately 1°C cooling (relative to today) from anthropogenic trace gas/aerosol changes. This model's sensitivity is relatively high, about 1.2°C $(\mathrm{W\ m^{-2}})^{-1}$, associated primarily with the amplifying effect of cloud cover changes. With a sensitivity half as large, hence more in the midrange of the Intergovernmental Panel on Climate Change (IPCC) estimates, the total cooling for this time period would then be about 0.75°C; this could be achieved in the model by altering for example the cloud optical thickness parameterizations (Yao and DelGenio 2002). Nevertheless, to be consistent with the Mann et al. (1999) reconstruction would require an even lower sensitivity,

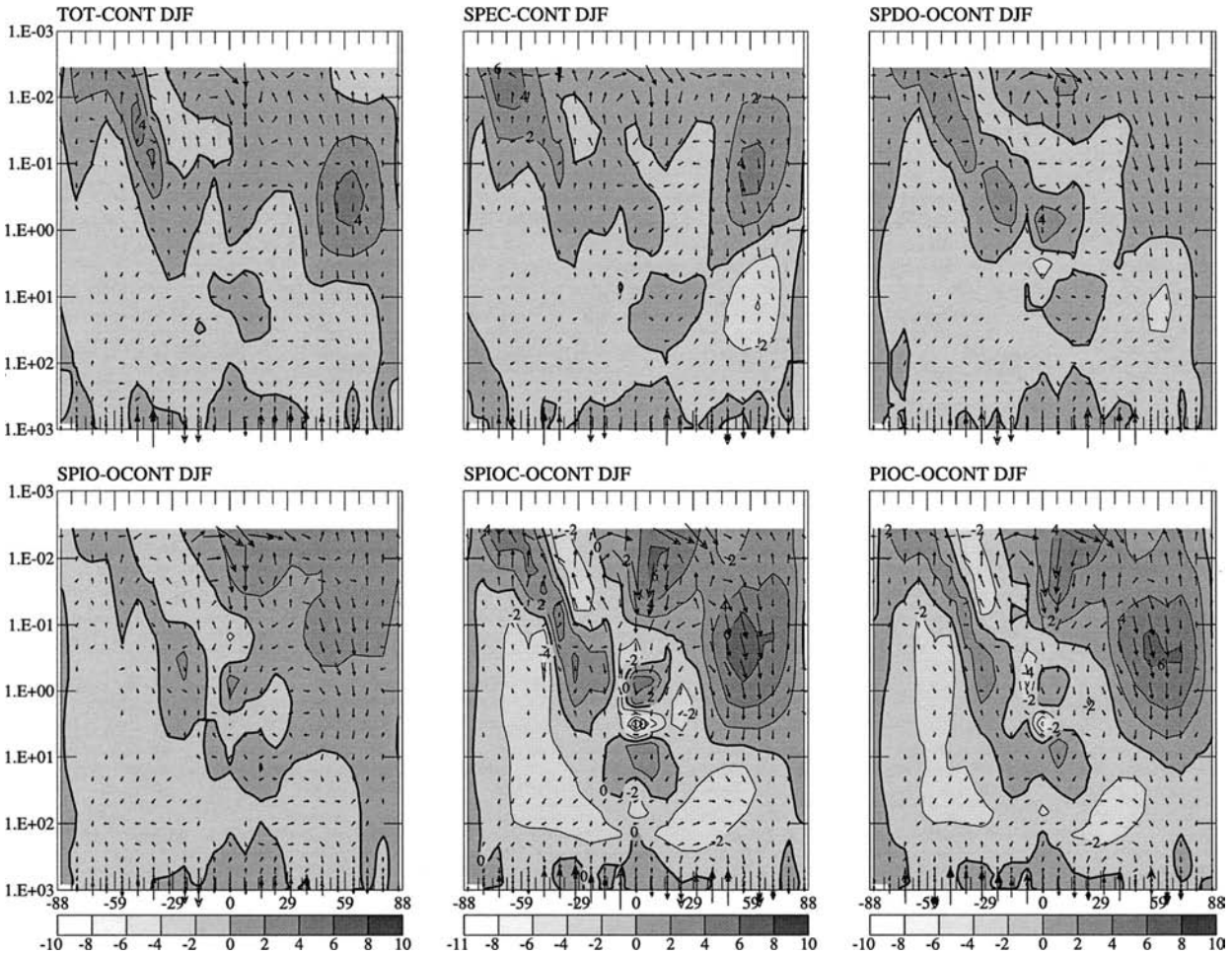

FIG. 6. Change in EP flux (arrows) and zonal wind in the different experiments during DJF.

of 0.4°C (W m^{-2})$^{-1}$; Crowley (2000) concluded that a sensitivity of 0.5°C (W m^{-2})$^{-1}$ matched the Mann et al. (1999) reconstruction when considering the whole record, not just the magnitude of Maunder Minimum cooling.

Not included in these experiments are potential volcanic aerosol effects. Different conclusions have been drawn by various researchers concerning the magnitude of stratospheric aerosols during the Maunder Minimum compared with current values. Robertson et al. (2001) reviewed some of the estimates, and using ice core data, produced a revised chronology that concluded that the Maunder Minimum time period had less highly explosive volcanoes than the latter half of the twentieth century, while global volcanic aerosol optical depths were somewhat similar. Robock and Free (1996) estimated that the optical depth was somewhat lower during the Maunder Minimum than in the last half century, while the dust veil index of Lamb (1983) and Crowley's (2000) reconstruction showed somewhat higher values [with a modified version noted as having uncertainty of ~50%; Hegerl et al. (2003)]. As indicated by these and other conflicting results, uncertainties in aerosol loading prevent us from knowing whether volcanoes significantly contributed to the cooling during the Maunder Minimum relative to today.

We also have ignored land albedo changes, which have been estimated to contribute 0.2°–0.4°C to preindustrial warming [the naturally occurring vegetation having a smaller surface albedo than currently exists; Hansen et al. (1998)]. An additional viewpoint suggests that the Maunder Minimum cooling is simply part of a natural millennial-scale climate oscillation that has been occurring over the last 0.5 million years (McManus et al. 1999; Bond et al. 2001); ocean dynamics changes are not allowed in these simulations.

In Fig. 2b we compare the temperature changes in the various experiments for the solar forcing in SPIO with several different reconstructions, including that estimated from borehole temperatures gridded to produce a global average (Briffa and Osborn 2002), by Esper et al. (2002; whose coldest period in their reconstruction

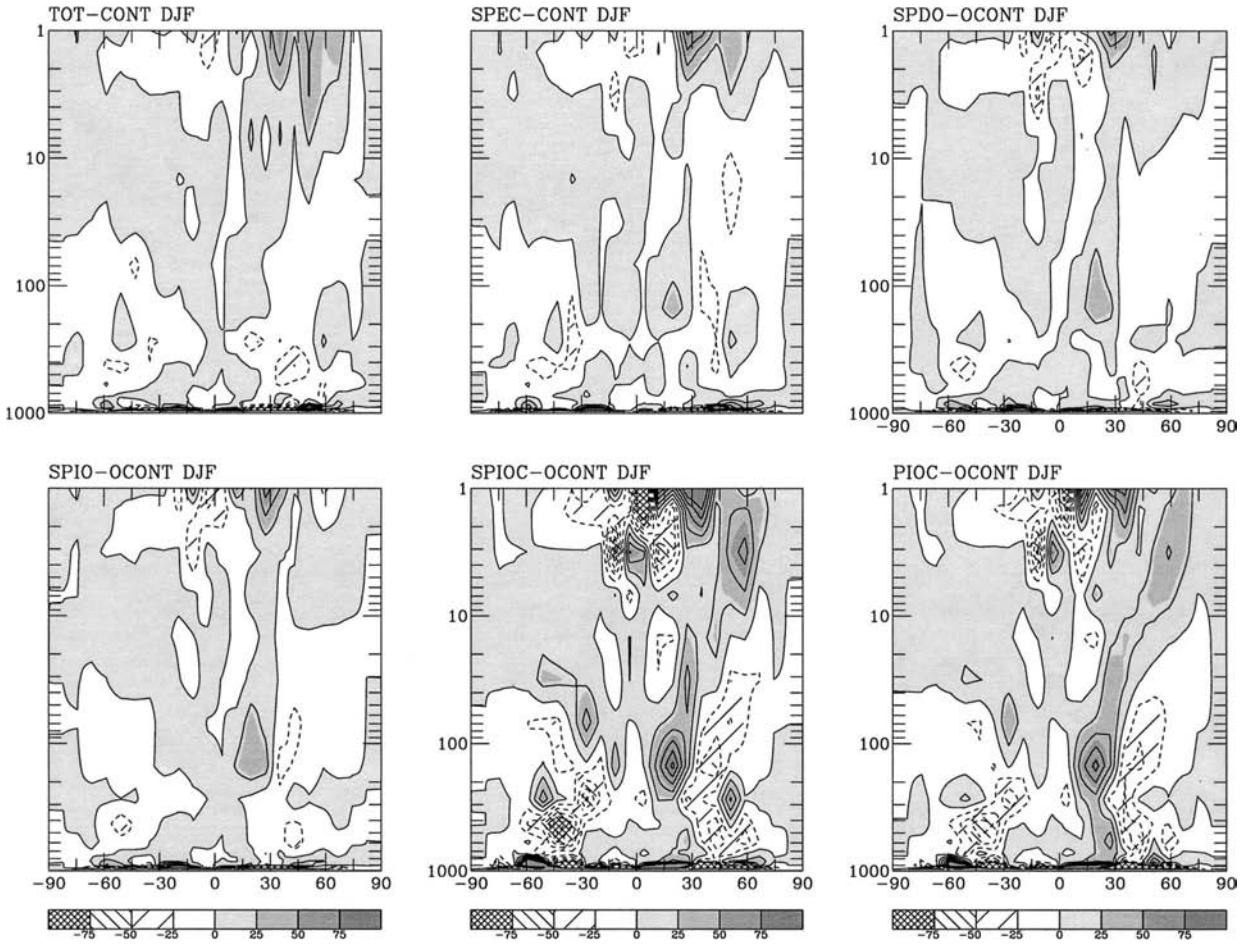

FIG. 7. Change in the EP flux divergence during DJF. Note the more limited vertical domain shown, compared with previous figures.

was actually before 1650, and whose results were more extratropical), and the smaller magnitude values obtained by Mann et al. (1998, 1999). While SPIO seems to be producing generally similar results to these sets of observations, this is with the solar forcing only, that is, without the much larger cooling that arises from the trace gas/aerosol changes. Such a situation is not unique to the GISS model. Cubash et al. (1997) using a larger estimate of total irradiance reduction (0.4%) and the ECHAM3 model with lower sensitivity also produced a cooling of about 0.5°C for this time period from solar effects alone. Fischer-Bruns et al. (2002) with the ECHAM4 model utilized trace gas/aerosol forcing similar in total radiation change to that used here, solar forcing about 1/2 that used in this study, and volcanic forcing greater than present day; their cooling for this time period averaged about −1°C, peaking at about −1.2°C. This value is greater than the cooling of about 0.6°C relative to the late 1990s found by Crowley (2000) using the same forcing in an energy balance model with a sensitivity of 0.5°C $(W\ m^{-2})^{-1}$. With the same model and multiple forcings, given the forcing used, the volcanic influence for the late Maunder Minimum was actually more important than the solar effect (Hegerl et al. 2003). Bauer et al. (2003) with a model of intermediate complexity [sensitivity of 0.65°C $(W\ m^{-2})^{-1}$] using solar forcing of −0.24% found cooling of about 0.5°C from that effect alone, and CO_2 forcing (of about 1.5 W m^{-2}) produced cooling of some 0.6°C; a deforestation warming of about 0.35°C was needed to make the results compare better with the Mann et al. reconstruction.

The discrepancy between GCM results, when all forcings are considered, and the estimates of the cooling magnitude indicates that either the paleoreconstructions underestimate what really happened, the climate forcings are overestimated, or the climate sensitivity is lower than that in most GCMs. Using the 17 models listed in Houghton et al. (2001) the average sensitivity is 0.86° ± 0.23°C $(W\ m^{-2})^{-1}$. To produce the estimated cooling in Mann et al. (1999) for this time (of about 0.4°C, or 1/4 of the GCM result in SPIOC), would require a sensitivity of about 0.3°C $(W\ m^{-2})^{-1}$. Uncertainties in estimates of anthropogenic and solar forcing are quite

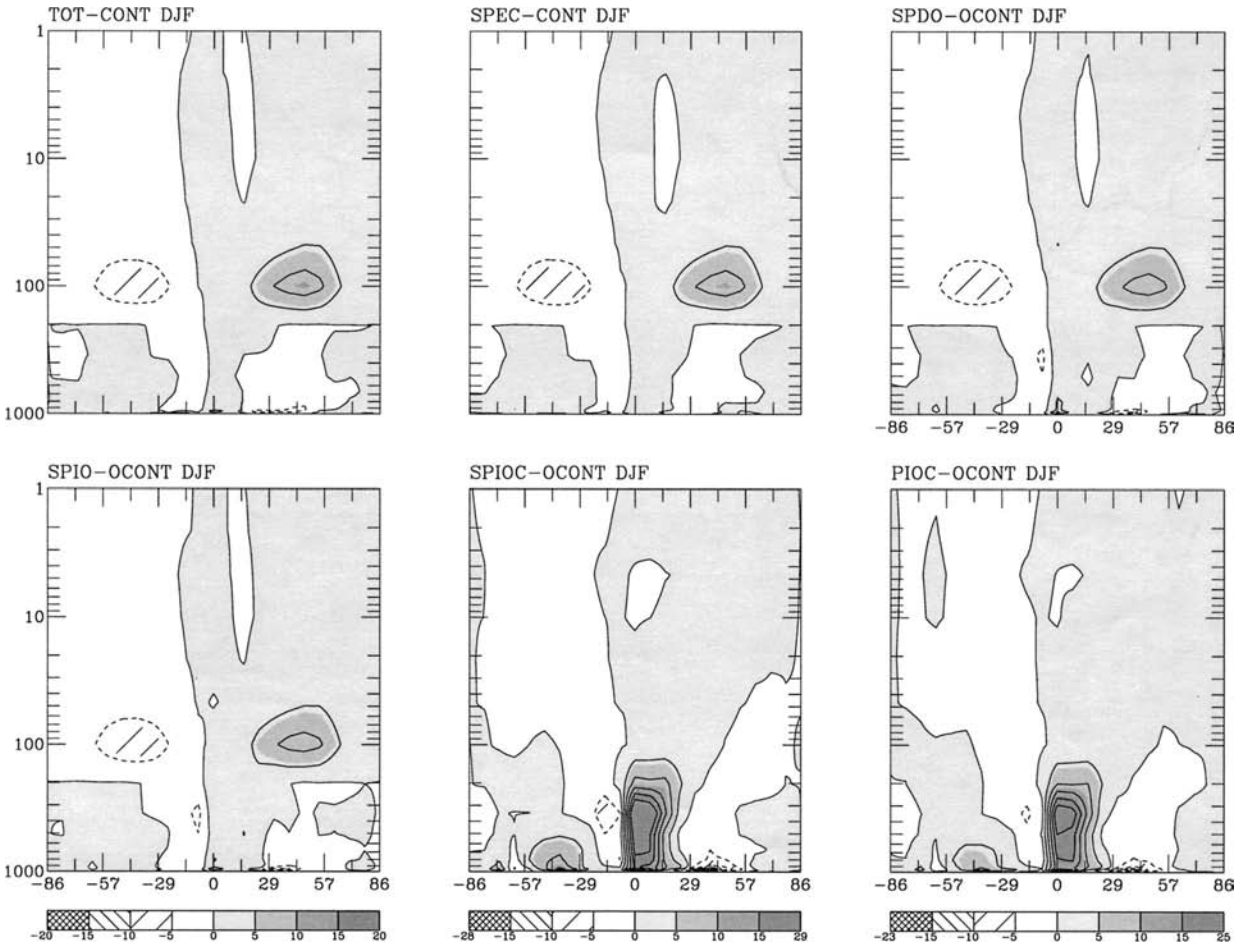

FIG. 8. Change in the transformed (residual) streamfunction. A positive change is a more indirect (counterclockwise) change in the Northern Hemisphere.

large, as discussed in the introduction, as is the deforestation effect used by Bauer et al. (2003), and possible volcanic influence. Model sensitivity can be varied by altering certain parameterizations, as noted above. The observations for this time period are very sparse, not only in the Tropics but also of the extratropical data used for EOF construction (and hence tropical reconstruction) in the Mann et al. studies (which also assumed unchanging EOF patterns).

b. Regional (circum-Atlantic) cooling during the Maunder Minimum

Shindell et al. (2001a), using the same model as employed here, suggested that the regional expression of the cooling during the Maunder Minimum compared to the late 1700s looked like that associated with the negative phase of the Arctic Oscillation, which was generated in the model by solar forcing in conjunction with the ozone response. That study also concluded that the Maunder Minimum ozone change (in that case an increase in the upper stratosphere and a decrease in the lower stratosphere, when compared with the late 1700s) was a strong factor in the resulting negative AO phase. The experiments reported here when compared with the current climate found that the phase of the high-latitude circulation response (Table 3) for the NAO and AO is negative in experiments 3–8. The relative poleward EP flux seen at the highest latitudes (Fig. 6) is consistent with this result, as angular momentum is transported equatorward, so that a relative east wind increase occurs at high latitudes in conjunction with higher pressure. The EP flux meridional propagation change in turn results from the relative east wind increase in the extratropical troposphere, due to a reduction in the temperature gradient across midlatitudes. As discussed in Rind et al. (2002a), in this GISS model the extratropical latitudinal temperature change is strongly influenced by the Hadley cell response: with a decrease in the Hadley cell, as occurs in these experiments due to the tropical cooling, there is less energy convergence ~35°N in the upper troposphere, providing for cooling there, and

weakening the latitudinal gradient in the extratropics. (The tropical cooling itself weakens the upper-tropospehereric temperature gradient at lower latitudes.)

There is no indication that the solar changes were any more effective than the trace gas changes in inducing this negative phase, as both reduced the Hadley cell intensity (Fig. 8). The ozone response also did not appear crucial, although it appeared to have some influence: the NAO and AO changes based on EOFs were more statistically significant when ozone was decreasing in the lower stratosphere (SPDO). However, with strong enough cooling due to anthropogenic forcing, a negative change occurred with increased lower stratospheric ozone (SPIOC, PIOC). From this perspective, it is inconclusive whether a negative phase of the AO during the Maunder Minimum relative to today was the result of solar forcing or cooling by some other mechanism. Lutterbacher et al. (1999) reconstructed NAO values that show a generally negative phase (higher pressure over Iceland) for the entire time period from 1675 to 1850. This would then not appear to be directly from solar forcing, which is thought to have been relatively higher during the eighteenth century (Lean 2000). Volcanic activity may have been greater and promoting cooling during part of this time, although observations following major volcanoes suggest its direct impact is to promote a more positive phase of the AO (e.g., Graf et al. 1994).

c. Model dependence of the NAO/AO change

Included in Table 3 are the results from an equilibrium run with total solar irradiance reduced by 0.25% (hence similar to experiment 3, but with a 25% greater reduction) using a model which extends only to 10 mb. Its surface air temperature change was −0.45°C (Rind and Overpeck 1994) or slightly less than in experiment 3 due to a lower model sensitivity. The NAO phase change is now positive, and the AO phase change negligible. This result is consistent with the claim of Shindell et al. (1999a) that including a full stratosphere is necessary to obtain an AO response in climate change experiments, in particular the trend due to global warming, at least in this model. Also shown is the result from the same model with a 2% irradiance reduction, and an associated cooling of about 5°C. Now the NAO/AO response is clearly visible, indicating that when the forcing is sufficiently strong, the wind changes and the EP flux response will arise even with a model that lacks a properly resolved stratosphere. Gillet et al. (2002) found that raising the model top did not alter their AO response to doubled CO_2, so it does not necessarily have an impact. There is also little obvious tendency toward a negative AO phase in the shorter runs made with the finer-resolution model discussed below.

Considering other GCM studies, Fischer-Bruns et al. (2002) (in the ECHAM4 model without a full stratosphere) found that during their model cooling from 1671 to 1684, the NAO index was more negative while during a subsequent warming (1685–1708) it was more positive. Considering that the GISS model (and the observations) do not indicate the subsequent warming period, their results for the cooling phase are generally consistent with those shown in Table 3. Luterbacher et al. (1999) for the 1675–1700 time period show a generally negative NAO EOF with standardized values generally ranging between 0 and −0.7 for December–February, similar to the results in Table 3.

d. Ozone during the Maunder Minimum

As indicated in Table 2 and Fig. 4, our simulations suggest that ozone was increased during the Maunder Minimum and other preindustrial time periods due to the composition of the preindustrial atmosphere. We determine the solar influence by comparing SPIOC and PIOC which shows that reduced UV led to a reduction in ozone by 2.7% in the upper stratosphere, and a reduction in total stratospheric ozone by 1.4%. The total reduction was therefore the same as arose when using the current background atmosphere (SPDO). The experiments performed by Shindell et al. (2001a) found that the reduced UV during the Maunder Minimum caused ozone to *increase* in the upper stratosphere when compared with a preindustrial time period 100 years later when solar irradiance was higher. Note that those experiments did not allow the preindustrial atmosphere to affect the background stratospheric temperature (other than through its effect on ozone), as was allowed in experiments SPIOC and PIOC.

To determine the model dependency of these results, we compare them with those obtained by using a 4° × 5°, 53-layer version of the model with the Linoz photochemistry scheme included (see Rind et al. 2002b) which was augmented to allow the ozone to respond to UV variations as well as overhead ozone column, temperature, water vapor, chlorine, and N_2O. Simulations were performed by using the sea surface temperature changes developed in the experiments with the coarser grid model for this time period, while altering the solar radiation in the fashion employed for runs 4–7. The experiments were done both with and without online transport, for better comparison with the ozone approach used in the coarser grid model. The simulations were run for 12 yr, and results are shown for the last 10 yr.

The relevant ozone changes are given in Fig. 10, which can be related to the results in Fig. 5 and Table 2. In comparison with SPDO, with no tracer transport (Fig. 10, top left), the Linoz scheme resulted in qualitatively similar responses, with ozone reduction in the upper stratosphere (−0.5% at 0.7 mb, hence, less than in the Shindell et al. scheme) and reduction in total ozone (−1.5%, in agreement with the Shindell et al. scheme). When transports were included (Fig. 10, bottom left), the changes were slightly less (−0.3% and −1.2%, respectively). As can be seen in the figures, the

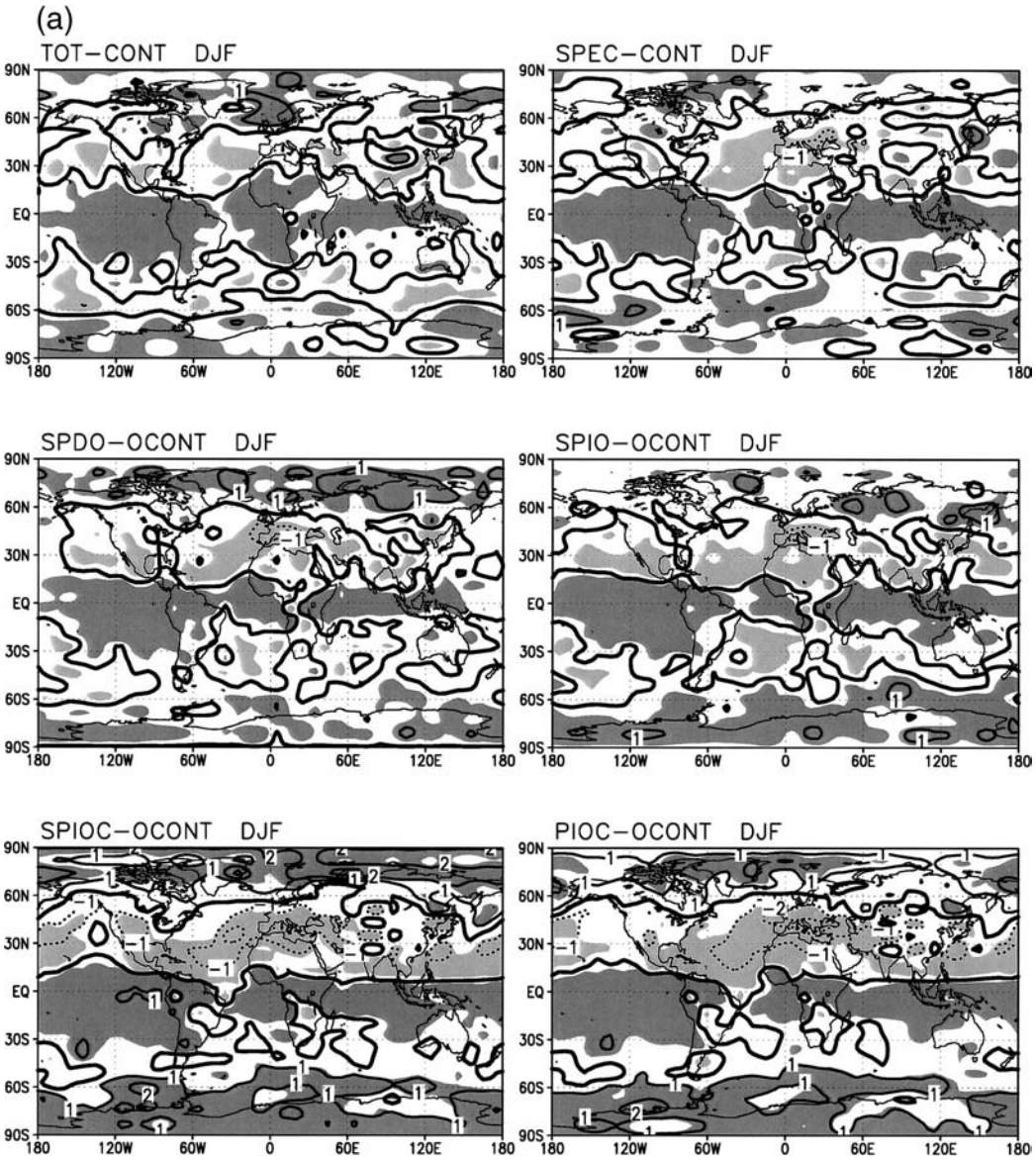

FIG. 9. (a), (b) Change in sea level pressure for the solstice seasons in the different experiments. The heavy black line indicates the zero contour. Increases (decreases) that are significant at the 95% level are shown by the dark (light) shading.

inclusion of transport resulted in increased ozone in the tropical lower stratosphere, due to a reduction in the transport of air with low-tropospheric ozone from the troposphere. This effect is somewhat overestimated, since the only tropospheric ozone included here was that which came from the stratosphere, though reduced tropospheric ozone in the preindustrial world would also influence these results. The reduced tropical upwelling is driven by the cooling, and is similar to the reduced tropical residual circulation change shown in Fig. 8.

In comparison with experiment SPIO, without transport (Fig. 10, top right) the results were again qualitatively similar: ozone increased both in the upper stratosphere (3.4% at 0.7 mb), and total (1.6%), although with smaller values than reported in Table 3. When transport was included (Fig. 10, bottom right), the upper-stratosphere change dominated by photochemistry was similar (3.4%) but total ozone now decreased (−1%), due to the more negative values in the lower stratosphere. As noted earlier, the preindustrial atmosphere's increased ozone in the upper stratosphere/lower mesosphere absorbed more UV radiation at those levels, reducing the amount penetrating to the midstratosphere. This amplified the UV reduction to the midstratosphere already occurring during the Maunder Minimum, and resulted in decreased ozone there. The effect

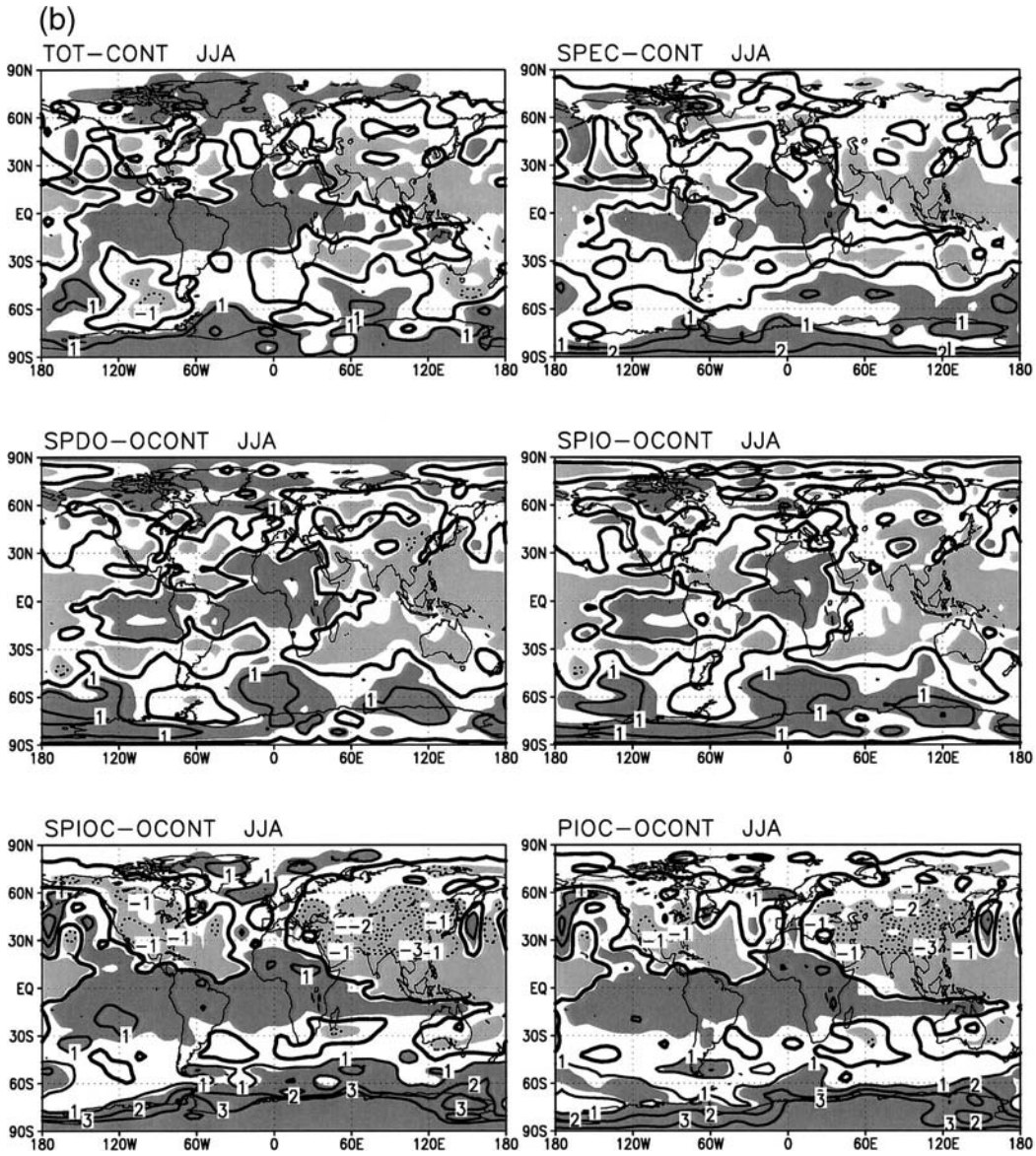

FIG. 9. (*Continued*)

was then translated downward due to the reduced tropical upwelling.

We can also test the results of Shindell et al. (2001a). With the Maunder Minimum UV reduction in the preindustrial atmosphere compared with the current solar in a preindustrial atmosphere, there is a small increase in upper-stratospheric and total ozone (1% and 0.3%, respectively) without transports included, thus qualitatively similar to the previous model results. However, with transport, total ozone now decreases (−0.2%) as discussed above for SPIO.

Overall, then, the Linoz scheme qualitatively reproduces the effect of solar and anthropogenic gases calculated by the Shindell et al. scheme, especially without transports. Note that in general the Linoz scheme results in smaller increases due to the preindustrial atmosphere than the Shindell et al. scheme. Wuebbles et al. (1998) calculated even larger percentage increases in the upper-stratosphere polar regions. The reason(s) for these differences will be the subject of future research.

5. Conclusions

Experiments were undertaken to address the relative influences of solar spectral versus total irradiance changes for the Maunder Minimum time period, the possible influence of stratospheric ozone changes during this time, the relative importance of anthropogenic and solar

TABLE 4. Regional annual changes in several of the simulations. Significant results (95% level) are given in bold type.

	SPIO			SPIOC			PIOC		
Region	ΔT(°C)	ΔP%	ΔSM%	ΔT(°C)	ΔP%	ΔSM%	ΔT(°C)	ΔP%	ΔSM%
W-US	**−.49**	−2.1	2.5	**−.8**	**−16.7**	**−22**	**−.45**	**−12.0**	**−15.6**
MID-US	**−.52**	0.9	−0.1	**−.95**	**−4.8**	**−7.5**	**−.45**	0.0	−6.1
E-US	**−.44**	−2.9	−0.6	**−1**	3.7	6.1	**−.6**	1.9	5.5
S-CAN	**−.54**	**−4.7**	−3.4	**−.5**	**−12.5**	**−22.8**	**−.45**	**−7.1**	**−15.4**
GRNLND	**−.65**	−0.6	0.0	**−1.3**	**−7.1**	0.3	**−.95**	−3.4	0.2
MID-EUR	**−.56**	−2.4	**−3.1**	**−.85**	**−9.1**	**−24.0**	**−.5**	**−6.7**	**−18.6**
NOR-RUS	**−.55**	**−5.9**	**−16**	**−.95**	**−15.1**	**−52.6**	**−.4**	**−11.7**	**−36.6**
W-SIBER	**−.73**	−2.9	0.8	**−1.4**	**−8.7**	**6.3**	**−.4**	**−8.7**	−2.7
SIB-PLAT	**−.76**	**−7.1**	0.8	**−1.1**	**−9.1**	**9.6**	**−.35**	**−4.3**	**4.0**
S-CHINA	**−.51**	−1.6	1.2	**−1.3**	0.0	**8.2**	**−.75**	0.0	**5.8**
CHINA-DES	**−.52**	−1.2	3.4	**−1**	0.0	6.8	**−.4**	−3.3	1.2
INDIA-DES	**−.41**	−2.1	4.2	**−.65**	−5.9	−5.9	**−.2**	−1.9	−0.8
AUSTR-DES	**−.72**	−0.9	**15**	**−2.3**	0.0	−6.3	**−1.8**	0.0	**11.4**
N-SAHARA	**−.67**	0.0	0.9	**−1.3**	**16.7**	**22.8**	**−.6**	**9.1**	**12.3**
S-SAHARA	**−.67**	−2.5	0.0	**−1.8**	**33.3**	**7.7**	**−1**	**33.3**	**7.7**
AFR-SAHEL	**−.75**	−1.3	9.3	**−2.4**	**9.1**	**28.9**	**−1.7**	**11.1**	**28.9**
AFR-RFOR	**−.58**	**−3.8**	−3.0	**−2.1**	**−4.1**	−3.5	**−1.5**	−1.0	**5.4**
AMAZ-RFO	**−.55**	**−1.7**	1.5	**−1.9**	0.0	**5.3**	**−1.4**	**2.7**	**7.7**

forcing for the Maunder Minimum time period compared with the current climate, and the effect of including a full stratosphere on the climatic responses, particularly the AO/NAO. The principal conclusions are the following.

Total versus spectral irradiance change:

- Compared with a uniform percentage irradiance reduction, the spectrally differentiated solar irradiance had more of its energy change in the UV, and thus somewhat less of a change in radiation entering the troposphere, but it did not produce a significantly different global tropospheric temperature response.
- With the uniform spectral irradiance reduction, there was a somewhat larger tropical–extratropical response and therefore a relatively smaller surface albedo change, effectively canceling out the incoming radiation difference.
- The spectrally discriminated irradiance change cooled the stratosphere much more than the uniform reduction.

Ozone response:

- The reduced solar UV irradiance led to stratospheric ozone reduction compared to today with both the current day background and preindustrial background.
- The preindustrial atmospheric composition produced a stratospheric ozone increase, which led to a total ozone increase during the Maunder Minimum.
- Using an alternate ozone photochemistry scheme (Linoz) in a higher-resolution model resulted in qualitatively similar responses except that the preindustrial composition effect was smaller, and advection changes altered the result in the equatorial lower stratosphere and polar regions.
- The ozone changes did not appear to have much influence on tropospheric climate or tropospheric atmospheric dynamics, with the possible exception of some effect on the high-latitude pressure/height indices.

Solar versus anthropogenic:

- With the magnitudes employed here (-0.68 W m^{-2} solar, -1.9 W m^{-2} anthropogenic), trace gas changes produced twice as much cooling (relative to today) as the solar irradiance change.
- The cooling is much larger than that estimated in some recent temperature reconstructions, and in particular, the tropical response is much greater.
- The NAO and AO phase is more negative due to either the anthropogenic or solar-induced cooling, associated with the tropical response and a Hadley cell intensity decrease, with greater changes when the cooling was greater.
- Precipitation changes followed the Hadley cell and NAO effects, and did not discriminate between the forcings outside of their different magnitudes.

Effect of including a full stratosphere:

- A full stratosphere was necessary to produce the negative NAO/AO response unless the cooling was sufficiently large.

The uncertainties in the relevant climate forcings (a factor of 8 for solar, and about 2 for anthropogenic) for this time period, and in the actual climate response, prevent any study at this time from being definitive. If both the solar forcing and anthropogenic changes used here are accurate, even without considering the possibility of increased volcanic aerosol emissions (offset to a some degree by land surface changes), then the climate

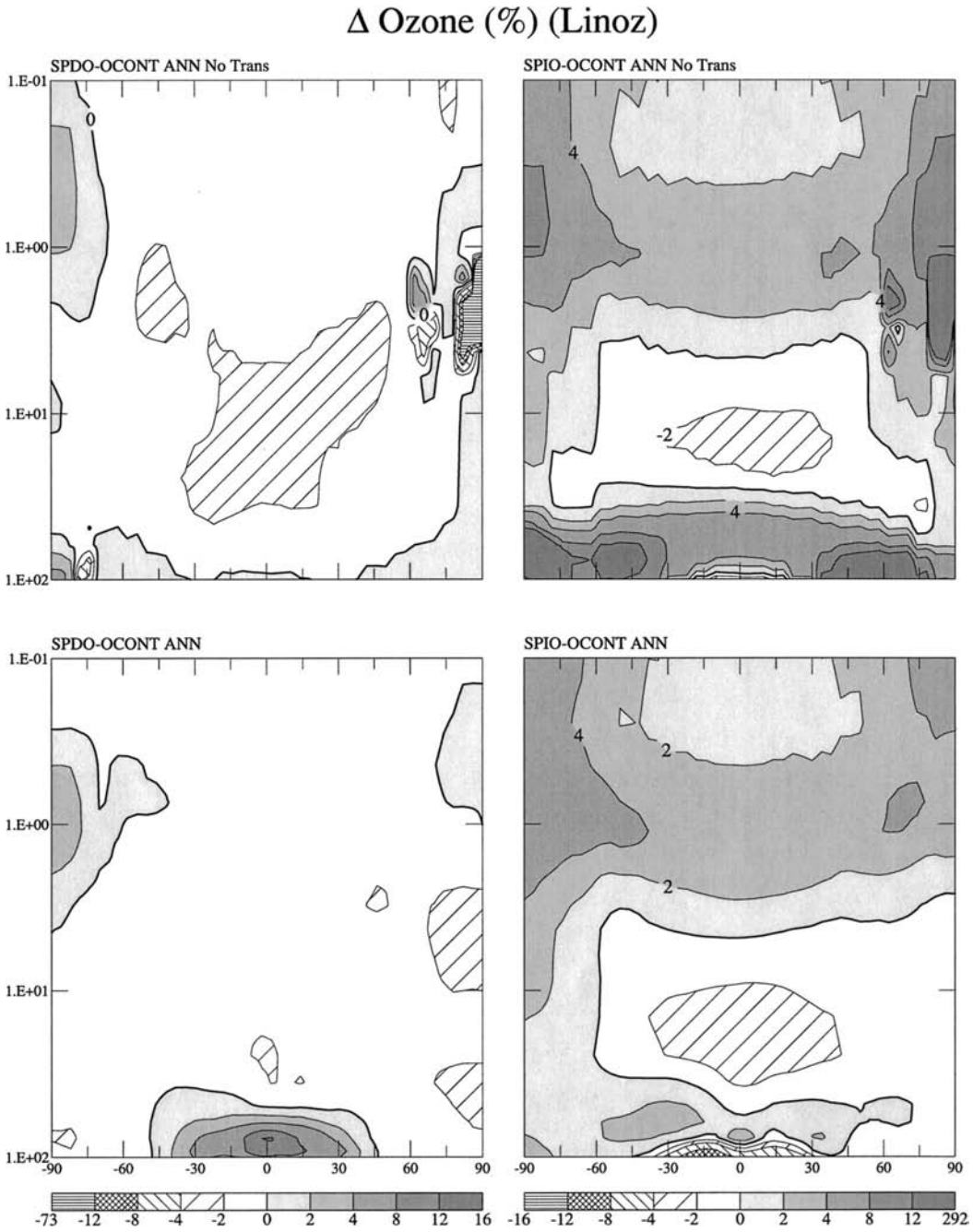

FIG. 10. Change in ozone using the Linoz photochemical code in the 4° × 5°, 53-layer model. Results shown are ozone changes corresponding to (left) SPDO and (right) SPIO, with (top) no transport, and (bottom) including transport.

sensitivity would have to be smaller than in this model by a factor of 4 to produce the limited response seen in some recent reconstructions. Uncertainty in the actual tropical sensitivity affects the reconstructions, and also affects our understanding of climate change in other time periods (ice ages, tertiary climates, and the future climate).

The relationship between natural and anthropogenic forcings is highlighted in this time period when compared with today, with questions concerning whether solar activity changes really alter solar irradiance, and what impact anthropogenic aerosol changes have really had on the radiation balance. The Maunder Minimum epoch therefore represents a crucible for understanding many of the top priority issues in climate change research.

Acknowledgments. This work was supported by the NASA Living With a Star program and by the NASA/ACMAP program for stratospheric–climate modeling. Climate modeling, in general, at GISS is supported by the NASA Climate Program.

REFERENCES

Bauer, E., M. Claussen, and V. Brovkin, 2003: Assessing climate forcings of the Earth system for the past millennium. *Geophys. Res. Lett.*, **30**, 1276, doi:10.1029/2002GL016639.

Beer, J., and Coauthors, 1994: Solar variability traced by cosmogenic isotopes. *The Sun as a Variable Star*, J. M. Pap et al., Eds., Cambridge University Press, 291–300.

Bond, G., and Coauthors, 2001: Persistent solar influence on North Atlantic climate during the Holocene. *Science,* **294,** 2130–2136.

Briffa, K. R., and T. J. Osborn, 2002: Blowing hot and cold. *Science,* **295,** 2227–2228.

Crowley, T., 2000: Causes of climate change over the past 1000 years. *Science,* **289,** 270–277.

Cubasch, U., R. Voss, G. C. Hegerl, J. Waszkewitz, and T. Crowley, 1997: Simulation of the influence of solar radiation variations on the global climate with an ocean-atmosphere general circulation model. *Climate Dyn.,* **13,** 757–767.

D'Arrigo, R., G. Jacoby, M. Free, and A. Robock, 1999: Northern Hemisphere temperature variability for the past three centuries: Tree-ring and model estimates. *Climate Change,* **42,** 663–675.

Eddy, J., 1976: The Maunder Minimum. *Science,* **192,** 1189–1202.

Esper, J., E. R. Cook, and F. H. Schweingruber, 2002: Low-frequency signals in long tree-ring chronologies for reconstructing past temperature variability. *Science,* **295,** 2250–2253.

Fischer-Bruns, I. F., U. Cubasch, H. von Storch, E. Zorita, J. F. Gonzales-Rouco, and J. Luterbacher, 2002: Modeling the late Maunder Minimum with a 3-dimensional ocean-atmosphere GCM. *CLIVAR Exch.,* **7,** 59–61.

Foukal, P., and L. Milano, 2001: A measurement of the quiet network contribution to solar irradiance variation. *Geophys. Res. Lett.,* **28,** 883–886.

Gillett, N. P., M. R. Allen, and K. D. Williams, 2002: The role of stratospheric resolution in simulating the Arctic Oscillation response to greenhouse gases. *Geophys. Res. Lett.*, **29**, 1500, doi:10.1029/2001GLO14444.

Graf, H. F., J. Perlwitz, and I. Kirchner, 1994: Northern Hemisphere tropospheric mid-latitude circulation after violent volcanic eruptions. *Contrib. Atmos. Phys.*, **67,** 3–13.

Haigh, J. D., 1996: The impact of solar variability on climate. *Science,* **272,** 981–984.

Hansen, J., A. Lacis, D. Rind, G. Russell, P. Stone, I. Fung, R. Ruedy, and J. Lerner, 1984: Climate sensitivity: Analysis of feedback mechanisms. *Climate Processes and Climate Sensitivity*, J. Hansen and T. Takahashi, Eds., *Geophys. Monogr.*, No. 29, Amer. Geophys. Union, 130–163.

——, M. Sato, A. Lacis, R. Ruedy, I. Tegen, and E. Matthews, 1998: Climate forcings in the industrial era. *Proc. Natl. Acad. Sci.*, **95,** 12 753–12 758.

Hegerl, G. C., T. J. Crowley, S. K. Baum, K.-Y. Kim, and W. T. Hyde, 2003: Detection of volcanic, solar and greenhouse gas signals in paleo-reconstructions of Northern Hemispheric temperature. *Geophys. Res. Lett.*, **30**, 1242, doi:10.1029/2002GL016635.

Houghton, J. T., Y. Ding, D. J. Griggs, M. Naguer, P. J. van der Linden, and D. Xiaosu, Eds., 2001: *Climate Change 2001: The Scientific Basis.* Cambridge University Press, 881 pp.

——, L. G. Meira Filho, B. A. Callander, N. Harris, A. Kattenberg, and K. Maskell, Eds., 1996: *Climate Change 1995. The Science of Climate Change.* Cambridge University Press, 572 pp.

Hoyt, D. V., and K. H. Schatten, 1993: A discussion of plausible solar irradiance variations, 1700–1992. *J. Geophys. Res.,* **98,** 18 895–18 906.

Jacoby, G., and R. D'Arrigo, 1989: Reconstructed Northern Hemisphere annual temperature since 1671 based on high-latitude tree-ring data from North America. *Climate Change,* **14,** 39–59.

Lamb, H. H., 1983: Update of the chronology of assessments of the volcanic dust veil index. *Climate Monit.,* **12,** 79–90.

Larkin, A., J. D. Haigh, and S. Djavidnia, 2000: The effect of solar irradiance variations on the earth's atmosphere. *Space Sci. Rev.,* **94,** 199–214.

Lean, J., 2000: Evolution of the sun's spectral irradiance since the Maunder Minimum. *Geophys. Res. Lett.,* **27,** 2425–2428.

——, and D. Rind, 1998: Climate forcing by changing solar radiation. *J. Climate,* **11,** 3069–3094.

——, Y.-M. Wang, and R. Sheely Jr., 2002: The effect of increasing solar activity on the Sun's total and open magnetic flux during multiple cycles: Implications for solar forcing of climate. *Geophys. Res. Lett.,* **29**, 2224, doi:10.1029/2002GL015880.

Luterbacher, J., C. Schmutz, D. Gyalistras, E. Xoplaki, and H. Wanner, 1999: Reconstruction of monthly NAO and EU indices back to A.D. 1675. *Geophys. Res. Lett.,* **26,** 2745–2748.

Mann, M. E., R. S. Bradley, and M. K. Hughes, 1998: Global-scale temperature patterns and climate forcing over the past six centuries. *Nature,* **392,** 779–787.

——, ——, and ——,1999: Northern Hemisphere temperatures during the past millennium: Inferences, uncertainties, and limitations. *Geophys. Res. Lett.,* **26,** 759–762.

——, and Coauthors, 2003: On past temperatures and anomalous late-20th century warmth. *EOS, Trans. Amer. Geophys. Union,* **27,** 256–257.

McCormack, J. P., and L. L. Hood, 1996: Apparent solar cycle variations of upper stratospheric ozone and temperature: Latitude and seasonal dependencies. *J. Geophys. Res.,* **101,** 20 933–20 945.

McHargue, L. R., and P. E. Damon, 1991: The global beryllium 10 cycle. *Rev. Geophys.,* **29,** 141–158.

McLinden, C. A., S. C. Olsen, B. Hannegan, O. Wild, M. J. Prather, and J. Sundet, 2000: Stratospheric ozone in 3-D models: A simple chemistry and the cross-tropopause flux. *J. Geophys. Res.,* **105,** 14 653–14 665.

McManus, J. F., D. W. Oppo, and J. L. Cullen, 1999: A 0.5 million-year record of millennial-scale climate variability in the North Atlantic. *Science,* **283,** 971–974.

Meehl, G. A., W. M. Washington, T. M. L. Wigley, J. M. Arblaster, and A. Dai, 2003: Solar and greenhouse gas forcing and climate response in the twentieth century. *J. Climate,* **16,** 426–444.

Rind, D., and J. Overpeck, 1994: Hypothesized causes of decade-to-century-scale climate variability: Climate model results. *Quat. Sci. Rev.,* **12,** 357–374.

——, R. Suozzo, N. K. Balachandran, A. Lacis, and G. L. Russell, 1988: The GISS Global Climate/Middle Atmosphere Model. Part I: Model structure and climatology. *J. Atmos. Sci.,* **45,** 329–370.

——, D. Shindell, P. Lonergan, R and N. K. Balachandran, 1998: Climate change and the middle atmosphere. Part III: The doubled CO_2 climate revisited. *J. Climate,* **11,** 876–894.

——, J. Lean, and R. Healy, 1999: Simulated time-dependent climate response to solar radiative forcing since 1600. *J. Geophys. Res.,* **104,** 1973–1990.

——, P. Lonergan, N. K. Balachandran, and D. Shindell, 2002a: $2\times CO_2$ and solar variability influences on the troposphere through wave–mean flow interactions. *J. Meteor. Soc. Japan,* **80,** 863–876.

——, J. Perlwitz, J. Lerner, C. McLinden, and M. Prather, 2002b: Sensitivity of tracer transports and stratospheric ozone to sea surface temperature patterns in the doubled CO_2 climate. *J. Geophys. Res.*, **107**, 4800, doi:10.1029/2002JD002483.

Robertson, A., and Coauthors, 2001: Hypothesized climate forcing time series for the last 500 years. *J. Geophys. Res.,* **106,** 14 783–14 803.

Robock, A., and M. P. Free, 1996: The volcanic record in ice cores

for the past 2000 years. *Climate Variations and Forcing Mechanisms for the Past 2000 Years*, P. D. Jones and R. S. Bradley, Eds., Springer-Verlag, 533–546.

Shindell, D., R. L. Miller, G. A. Schmidt, and L. Pandolfo, 1999a: Simulation of recent northern winter climate trends by greenhouse gas forcing. *Nature*, **399,** 452–455.

——, D. Rind, N. Balachandran, J. Lean, and P. Lonergan, 1999b: Solar cycle variability, ozone and climate. *Science*, **284,** 305–308.

——, G. Schmidt, M. Mann, D. Rind, and A. Waple, 2001a: Solar forcing of regional climate change during the Maunder Minimum. *Science*, **294,** 2149–2152.

——, ——, R. L. Miller, and D. Rind, 2001b: Northern Hemisphere winter climate response to greenhouse gas, ozone, solar and volcanic forcing. *J. Geophys. Res.*, **106,** 7193–7211.

Stuiver, M., and T. F. Braziunas, 1993: Sun, ocean, climate and atmosphere $^{14}CO_2$: An evaluation of causal and spectral relationships. *Holocene*, **3,** 289–305.

Wuebbles, D. J., C.-F. Wei, and K. O. Patten, 1998: Effects on stratospheric ozone and temperature during the Maunder Minimum. *Geophys. Res. Lett.*, **25,** 523–526.

Yao, M.-S., and A. D. Del Genio, 1999: Effects of cloud parameterization on the simulation of climate changes in the GISS GCM. *J. Climate*, **12,** 761–779.